



Long-term trends in aerosol properties derived from AERONET measurements

Zhenyu Zhang¹, Jing Li¹, Huizheng Che², Yueming Dong¹, Oleg Dubovik³, Thomas Eck^{4,5}, Pawan Gupta⁴, Brent Holben⁴, Jhoon Kim⁶, Elena Lind⁴, Trailokya Saud⁷, Sachchida Nand Tripathi⁷, and Tong Ying¹

¹Laboratory for Climate and Ocean-Atmosphere Studies, Department of Atmospheric and Oceanic Sciences, School of Physics, Peking University, 100871, Beijing, China

²State Key Laboratory of Severe Weather & Key Laboratory of Atmospheric Chemistry, Chinese Academy of Meteorological Sciences, China Meteorological Administration, 100081, Beijing, China

³Laboratoire d'Optique Atmosphérique, CNRS/Université de Lille, Villeneuve-d'Ascq, 59650, France

⁴NASA Goddard Space Flight Center, Greenbelt, 20771 MD, USA

⁵Goddard Earth Sciences and Technology Center, University of Maryland Baltimore County, Baltimore, MD, USA

⁶Department of Atmospheric Science, Yonsei University, Seoul, 03722, Republic of Korea

⁷Indian Institute of Technology Kanpur, Kanpur, 208016, India

Correspondence: Jing Li (jing-li@pku.edu.cn)

Abstract.

Over the past two decades, remarkable changes in aerosol compositions have been observed worldwide, especially over developing countries, potentially resulting in considerable changes in aerosol properties. The Aerosol Robotic Network (AERONET) offers high precision measurements of aerosol optical parameters over about 1700 stations globally, many of which have long-term measurements for one or more decades. Here we use AERONET Level 2.0 quality assured measurements to investigate long-term trends for aerosol optical depth (AOD) and Ångström exponent (AE) trends, and quality-controlled Level 1.5 inversion products to analyze trends of absorption aerosol optical depth (AAOD) and single scattering albedo (SSA) at stations with long-term records. We also classify the aerosol properties in these sites into 6 types, and analyze the trends of each type. Results reveal decreases in AOD over the majority of the stations, except for North India and the Arabian Peninsula, where AOD increased. AE also decreased in Europe, eastern North America, and the Middle East, but increased over South Asia and East Asia. The decreased AE over Europe and eastern North America is likely due to decreased fine-mode anthropogenic aerosols, whereas that over the Arabian Peninsula is attributed to increased dust activities. Conversely, increased AE over North India is probably attributed to increased anthropogenic emissions and decreased dust loading. Most stations in Europe, North America, East Asia, and South Asia exhibit negative trends in AAOD, whereas Solar_Village in the Arabian Peninsula has positive trends. SSA at most stations increases and exhibits opposite trends to AAOD, but with several stations in central Europe and North America showing decreased SSA values. Trend analysis of different aerosol types further reveals the changes of different aerosol components that are related to AOD, AE, AAOD, and SSA trends. Stronger reductions in fine-mode absorbing species than that of non-absorbing aerosols are found over Europe and East Asia, whereas in eastern North America the reductions of aerosols are dominated by non-absorbing species. Increased aerosols in Kanpur over North India should be mainly comprised



20 of scattering species, whereas those in Solar_Village over the Arabian Peninsula are mainly dust. Weak seasonality is found in the trends of all aerosol parameters analyzed in this work.

1 Introduction

Aerosols are pivotal in the study of climate change due to their significant effects on the climate system. Understanding the climate effects of aerosols necessitates a comprehensive recognition of their optical and microphysical properties. Variations in aerosol loading and aerosol properties can result in disparate climate impacts, underscoring the importance of accurately comprehending these changes. For example, changes in aerosol loading can directly influence the intensity of aerosol forcing, while a rise in aerosol absorption could even shift the aerosol forcing from negative to positive (Hansen et al., 1997), remarkably altering their climate effects. To quantify the contribution of aerosols to climate variability effectively, it is thus crucial to understand and quantify the long-term change of aerosol properties.

30 Studies using satellite observations revealed continuous reductions in the loading of aerosols and their precursors in Europe, North America, South America, and Africa in the past several decades, but increases over South Asia and Middle East, as well as increases in 2000s and decreases in 2010s over East Asia (Krotkov et al., 2016; Mehta et al., 2016; Zhao et al., 2017; de Meij et al., 2012; Fioletov et al., 2023; Gupta et al., 2022). In situ measurements also suggested negative scattering and absorption coefficient trends in majority of the stations which mainly located in Europe and North America, and revealed positive trends of aerosol scattering (represented by single scattering albedo, SSA) in Asia, eastern/northern Europe, and the Arctic, and negative SSA trends in central Europe and central North America (Collaud Coen et al., 2020). As satellite observations may have drifts in long-term calibration which impact aerosol monitoring and mainly provide aerosol loading products, and the spatial coverage of in situ measurements is quite limited, ground-based remote sensing networks provide a very accurate data source to analyze trends in multiple aerosol parameters worldwide. Xia (2011) examined 79 stations within the Aerosol Robotic Network (AERONET, Holben et al., 1998) with observations no less than six years, and found decreases in aerosol optical depth (AOD) and Ångström exponent (AE) in eastern North America and Europe. Ningombam et al. (2019) analyzed long-term AOD trends over 49 AERONET sites and 4 Sky radiometer Network (SKYNET, Takamura and Nakajima, 2004) sites, and reported decline in AOD over North-South America, Europe, the Arctic, and Australia.

However, these studies based on ground-based remote sensing data mainly focused on trends in AOD and AE, while analysis on other aerosol optical properties, such as SSA and absorption aerosol optical depth (AAOD), is still insufficient. Other studies focusing on trends of these parameters are mainly restricted to specific stations with long-term records, which is mainly because of the limited data availability of AERONET Level 2.0 data. Li et al. (2014) utilized quality-controlled AERONET Level 1.5 inversion measurements at 54 selected stations as well as Level 2.0 solar observations at 90 selected stations worldwide for the period 2000-2013 to analyze the trends of AOD, AE, SSA, and AAOD. Decreased AOD and AAOD trends, along with increased SSA trends, were consistently observed in Japan, Europe and North America. North America exhibited positive AE trends, whereas Europe showed negative AE trends. India was reported to experience increases in AOD, AE, and SSA. The



Arabian Peninsula was noted for experiencing increased AOD and AAOD, with decreases in AE and SSA. Eastern China was characterized by a positive SSA trend and a negative AAOD trend, without significant changes in AOD or AE.

A decade later, many regions have experienced significant changes in aerosol loading and compositions. For example, recent studies have highlighted considerable reductions in aerosol loadings in East Asia as evidenced by AERONET measurements (Yu et al., 2022; Ramachandran and Rupakheti, 2022; Eom et al., 2022) and satellite observations (Ramachandran et al., 2020; Krotkov et al., 2016; Mehta et al., 2016; Zhao et al., 2017; Fioletov et al., 2023; Li, 2020; Gupta et al., 2022). Substantial reductions in anthropogenic emissions have been observed in eastern North America (Krotkov et al., 2016), potentially contributing to a decrease in AE. Central Australia has seen reported increases in dust activities (Shao et al., 2013), aligning with observed increases in AOD and decreases in AE (Yang et al., 2021), which might also lead to positive AAOD and negative SSA trends. Some potential variations in aerosol optical properties in certain regions were not captured by Li et al. (2014), partly due to limitations in the spatial and temporal coverages of surface stations at that time, and recent changes in aerosol loadings and compositions might lead to different or reversed trends. AERONET has now expanded from 400 to over 1700 stations globally with longer records. The AERONET algorithm has also been updated to Version 3 with numerous improvements (Giles et al., 2019; Sinyuk et al., 2020). These progresses underscore the need to update trend analysis of AERONET data to capture recent shifts in aerosol optical properties and reflect advancements in data quality and network coverage.

In this study, we analyze AERONET Level 2.0 AOD and AE observations at 165 stations and Level 1.5 quality-controlled AAOD and SSA measurements at 74 stations. We also made a further attempt to categorize aerosol types and analyze the trends of each type. We hope that this study can provide a more recent reference to aerosol changes globally and facilitate the assessment of aerosol climate and environmental impacts.

2 Data and Methods

2.1 AERONET Data

The AERONET is a ground-based aerosol remote sensing network, providing long-term observations of aerosol optical and microphysical properties, covering most of the continental areas around the world (Holben et al., 1998). The AERONET AOD observations are derived from direct solar radiation at several wavelength bands mainly ranging from 340 nm to 1640 nm, while other aerosol properties, including SSA and AAOD, are derived from diffuse sky radiance at four wavelengths at 440, 675, 870, and 1020 nm (Dubovik and King, 2000). The AE parameter is calculated using AOD measurements within 440–870 nm interval (Eck et al., 1999; Giles et al., 2019). There is a series of quality assurance strategies for AERONET Level 2.0 data that ensure an AOD uncertainty of 0.01 (visible)-0.02 (UV) and an SSA uncertainty of 0.03 at AOD₄₄₀ (AOD at 440 nm) \sim 0.4 (Holben et al., 2006; Giles et al., 2019; Sinyuk et al., 2020). However, as Level 2.0 quality assurance for inversion products requires a coincident AOD exceeding 0.4 at 440 nm, many stations do not have long-term Level 2.0 inversion records. Therefore, considering both the data quality and data availability, we utilize the all-point Version 3 Level 2.0 direct measurements for AOD and AE, and quality-controlled Level 1.5 almucantar inversion products (see below for the quality control scheme) for

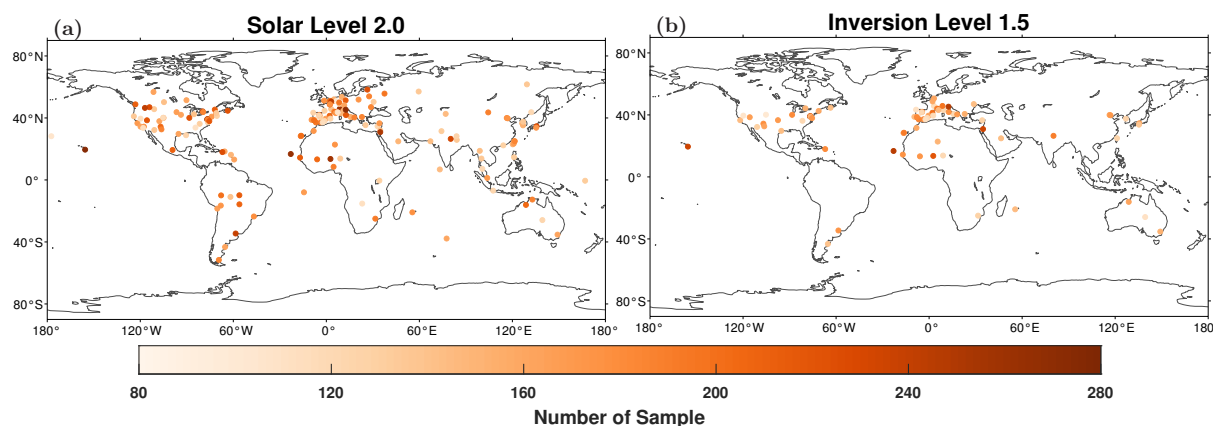


Figure 1. Locations of the stations selected for this study. (a) Level 2.0 solar stations, (b) Quality-controlled Level 1.5 almucantar stations. The number of monthly samples for each station is also displayed with different color.

other parameters. The uncertainty in SSA increases rapidly (exponentially) at lower AOD levels (Sinyuk et al., 2020), therefore
 85 much of the SSA retrievals in this study have larger uncertainties of ~ 0.03 to ~ 0.09 .

The stations are selected primarily based on the availability of an extensive data record for the purpose of estimating the
 long-term trends of aerosol properties. The Level 1.5 almucantar inversion products are first screened based on all the Level 2.0
 quality assurance criteria except for the AOD threshold, such as solar zenith angle $> 50^\circ$, sky error $< 5\%$, and coincident Level
 2.0 AOD measurements. The Level 2.0 direct measurements and screened Level 1.5 almucantar inversion products are then
 90 used to calculate monthly measurements. We calculate the median of all-point measurements to represent the monthly value
 only if there are more than 5 all-point measurements in at least 3 different days for that month. To ensure adequate records
 in trend analysis, we require the data to have at least 10 years of records and no less than 8 monthly measurements for each
 year during the 2000-2022 period. Specifically, the 2019-2022 data for Birdsville in Australia are eliminated for more accurate
 trend estimation, as these data are strongly biased due to a data filtering artifact in the quality assurance (QA) process of the
 95 algorithm according to Giles et al. (2019), which results in a large jump in AOD (personal communication, T. Eck). This AOD
 artifact is caused by erroneous time stamping of the data that is greatest at some sites in Australia due to a unique data logging
 system utilized there. The unnatural increase in AOD for Birdsville in 2019 can be found in Yang et al. (2021). As a result, 165
 stations for the direct-sun observations and 74 stations for the inversion measurements are retained for trend analysis, covering
 all major continents over the world. The distributions of all the selected stations as well as the number of monthly samples at
 100 each station are presented in Fig. 1. Locations of stations mentioned in the manuscript are presented in Fig. 2.

Here we focus on analyzing AOD, SSA, and AAOD trends at 440 nm, which are noted as AOD_{440} , SSA_{440} , and $AAOD_{440}$,
 respectively. Trends for parameters at the other wavelengths are very similar and thus skipped. The AE is calculated from AOD
 measurements within the 440–870 nm wavelength range (typically including 440, 500, 675, and 870 nm), and are commonly
 denoted as $AE_{440-870}$.

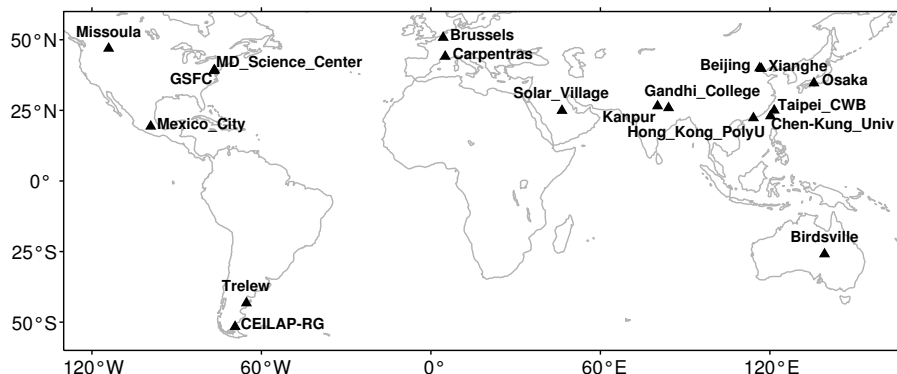


Figure 2. Locations of representative stations mentioned in the study.

105 2.2 Mann–Kendall test and Sen’s slope for trend analysis

Here we use the Sen’s slope combined with Mann–Kendall test to estimate the trend and its significance. The Mann–Kendall test (Mann, 1945; Kendall, 1975) is a nonparametric method to assess the significance of monotonic trends in a dataset without assuming any particular distribution. The slope of the trend k can be estimated by the median of the set of slopes (Sen, 1968):

$$k = \text{Median}\left(\frac{Y_j - Y_i}{t_j - t_i}\right), \forall j > i \quad (1)$$

110 where Y_i and Y_j are the values of the variable at times t_i and t_j , respectively.

The Sen’s slope is a robust measurement of the trend in a dataset, and is not sensitive to outliers. As aerosol optical parameters do not follow a normal distribution, and AERONET records often have missing data, the Sen’s slope is a good estimator of trends.

2.3 Aerosol Classification

115 In addition to the retrieved parameters, we also classify the observations into six aerosol types using the Fine Mode Fraction (FMF) at 550 nm and SSA at 440 nm (Lee et al., 2010). AOD and fine-mode AOD at 440, 675, 870, and 1020 nm are first interpolated to 550 nm using a second-order polynomial fit on a logarithmic scale (Eck et al., 1999). Then the FMF_{550} is calculated by AOD and fine-mode AOD at 550 nm. The classification criteria for the six aerosol types (Dust, Mixture, and four fine-mode types), as well as the proportion of each type in the total number of quality-controlled Level 1.5 all-point record, are listed in Table 1. It should be noted that sea salt aerosols that typically have FMF_{550} below 0.4 and SSA_{440} greater than 0.95 (denoted as the Uncertain type in Table 1) are not considered in this study, because most stations are located on the mainland and sea salt aerosols only account for a negligible proportion (about 2.5%).

Each quality-controlled Level 1.5 inversion all-point measurement is classified as a specific aerosol type according to the classification criteria in Table 1. Since the records for each aerosol type are usually too few to calculate a monthly value (i.e.,



Table 1. Criteria of aerosol classifications defined in Lee et al. (2010).

Aerosol type	FMF ₅₅₀	SSA ₄₄₀	Proportion
Dust	FMF ₅₅₀ < 0.4	SSA ₄₄₀ ≤ 0.95	14.4%
Mixture	0.4 ≤ FMF ₅₅₀ ≤ 0.6	/	17.2%
Non-absorbing Fine (NA)	FMF ₅₅₀ > 0.6	SSA ₄₄₀ > 0.95	22.6%
Slightly-absorbing Fine (SA)	FMF ₅₅₀ > 0.6	0.9 < SSA ₄₄₀ ≤ 0.95	21.6%
Moderately-absorbing Fine (MA)	FMF ₅₅₀ > 0.6	0.85 < SSA ₄₄₀ ≤ 0.9	11.4%
Highly-absorbing Fine (HA)	FMF ₅₅₀ > 0.6	SSA ₄₄₀ ≤ 0.85	10.3%
Uncertain	FMF ₅₅₀ < 0.4	SSA ₄₄₀ > 0.95	2.5%

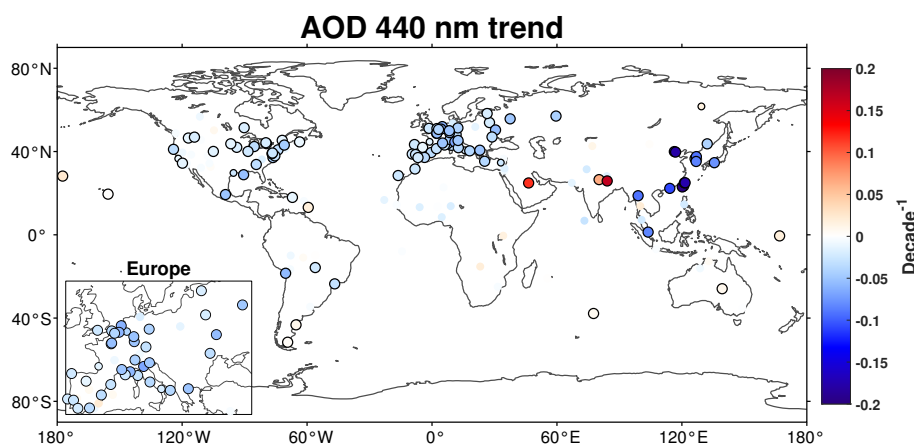


Figure 3. Trends of 440 nm AOD at AERONET stations. Dots without black boundary indicate trends below 90% significance level. Smaller dots with black boundary indicate trends at 90% significance, and larger dots with black boundary indicate trends at 95% significance. The magnitude of the trend has the unit of [per decade].

125 less than 5 measurements per month), we calculate the seasonal median values instead for the type analysis. Specifically, we use coincident Level 2.0 AOD₄₄₀ measurements to calculate the seasonal AOD and analyse its trend for each aerosol type.

3 Results

3.1 Trends for AOD and AE

130 The AOD₄₄₀ trends at the 165 selected AERONET stations are presented in Fig. 3. Trends surpassing the 90% significance level are marked with black circles, with larger dots denoting trends exceeding the 95% level. A global reduction of aerosol loading is found with most stations demonstrating significant negative AOD₄₄₀ trends, which is consistent with previous studies (Li et al., 2014; Xia, 2011; Ningombam et al., 2019). The AOD₄₄₀ time series at several representative sites are also shown

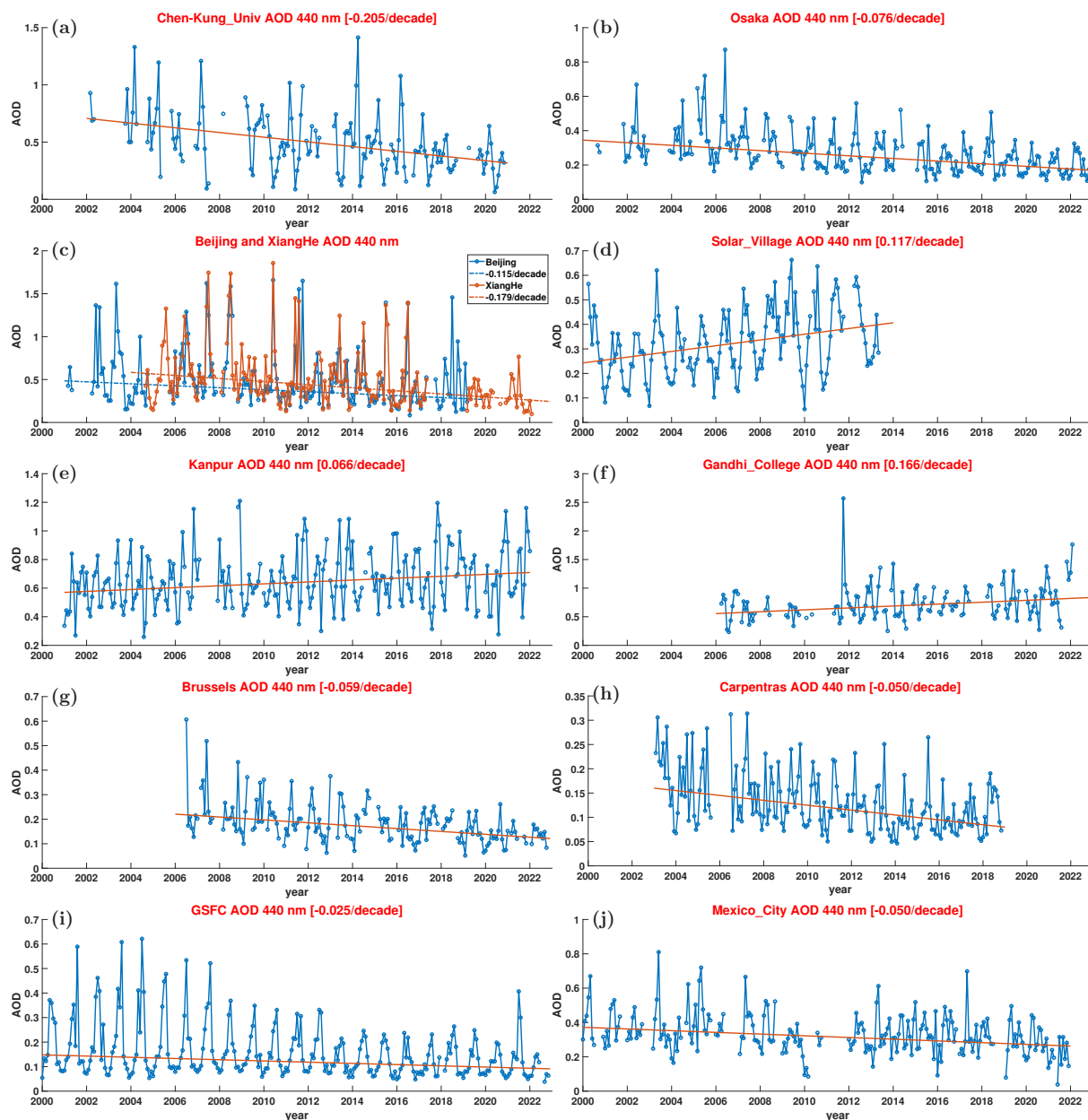


Figure 4. Time series of 440 nm AOD at several representative AERONET stations with trends at 95% significance. (a) Chen-Kung_ Univ, (b) Osaka, (c) Beijing and XiangHe, (d) Solar_Village, (e) Kanpur, (f) Gandhi_College, (g) Brussels, (h) Carpentras, (i) GSFC, (j) Mexico_City.

in Fig. 4. An increased number of stations with significant trends compared to these previous studies are observed in North America, Europe, and North Africa, likely due to spatial and temporal expansion of the network in recent years. The rates of AOD₄₄₀ reduction in western Europe are not as substantial as those reported in Li et al. (2014), suggesting a decelerating trend



of aerosol reduction in Europe in recent years. This is also in line with the AOD_{440} time series at representative European sites (Fig. 4g,h). Strong negative AOD_{440} trends are identified at more than 10 stations in East Asia and Southeast Asia, which were previously reported as exhibiting no significant trends in global studies (Li et al., 2014; Xia, 2011; Ningombam et al., 2019). The most considerable AOD_{440} reductions are observed in East China, with declines exceeding -0.1 per decade at all the five
140 stations (Chen-Kung_ Univ, XiangHe, Taipei_CWB, Beijing, and Hong_Kong_PolyU) and almost reaching -0.2 per decade at Chen-Kung_ Univ, XiangHe, and Taipei_CWB. East China was reported to have increased aerosol loading in 2000s (Yoon et al., 2012; de Meij et al., 2012; Ramachandran and Rupakheti, 2022), thus the substantial AOD reductions found in this study, which were also reported in regional studies employing recent records (Ramachandran and Rupakheti, 2022; Ramachandran et al., 2020; Yu et al., 2022; Eom et al., 2022; Li, 2020; Gupta et al., 2022), have occurred mainly in the last decade. Xianghe
145 and Beijing, two stations located very near to each other in East China, both possess Level 2.0 records spanning 19 years from 2000 to 2022 (Fig. 4c). However, the data record in Beijing, starting in 2001, reveals an AOD_{440} trend of -0.115 per decade, whereas that in Xianghe, starting in 2004, is more recent and exhibits a larger AOD_{440} decrease of -0.179 per decade, emphasizing the later years as a period of most notable AOD_{440} reduction.

Significant positive AOD_{440} trends are found over Kanpur and Gandhi_College in North India, Solar_Village in the Arabian
150 Peninsula, Birdsville in Australia, two stations in South America (Trelew and CEILAP-RG), and several oceanic island stations. Note that several of these sites (Birdsville, Trelew, CEILAP-RG, and some oceanic sites) have very low AOD_{440} (typically below 0.1 for monthly values) as well as low AOD_{440} variability, therefore the results in these stations are typically more uncertain. The Level 2.0 AOD_{440} records at Solar_Village (Fig. 4d) ended in 2013, limiting current insights into aerosol properties in the Arabian Peninsula. Kanpur (Fig. 4e) has extensive records over the past two decades, exhibiting a positive
155 AOD_{440} trend of 0.060 per decade. This value is close to the trends calculated from different periods in previous studies (Ramachandran and Rupakheti, 2022; Li et al., 2014; Kaskaoutis et al., 2012; Kumar et al., 2022), indicating a steady increase in AOD_{440} there. Compared to previous global studies, an additional station named Gandhi_College (Fig. 4f) in northern India is observed to have a significant positive AOD_{440} trend of 0.149 per decade, indicating a more pronounced increase in aerosol loading in this region. Positive AERONET AOD_{440} trends over the other regions are generally weaker, with magnitudes
160 typically below 0.03 per decade. The positive AOD trend for Birdsville in Australia was confirmed by the independent research conducted by Yang et al. (2021), however this was a false trend resulting from a previously mentioned data screening anomaly. Hsu et al. (2012) also suggested an increase in oceanic AOD , consistent with the widespread positive trends at oceanic stations.

The $AE_{440,870}$ parameter characterizes the wavelength dependency of AOD and closely correlates with aerosol particle size distribution. Dust particles typically have $AE_{440,870}$ values around 0.3 or lower, and the $AE_{440,870}$ for fine-mode particles that
165 are mostly anthropogenic, usually exceed 1.0 (Farahat et al., 2016; Giles et al., 2012; Russell et al., 2010; Dubovik et al., 2002). Therefore, $AE_{440,870}$ can reflect the relative fraction of fine and coarse mode particles. The error in AE can be estimated by

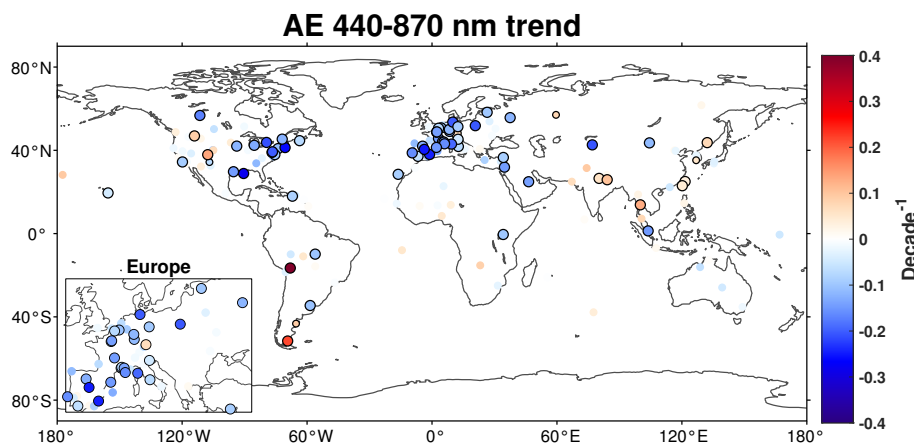


Figure 5. Same as Fig. 3, but with trends of AE.

the error in AOD as (Li et al., 2014; Kato et al., 2000):

$$\Delta AE = \left[\frac{\sum_{i=1}^n e_i^2}{(n-2) \sum_{i=1}^n (\ln \lambda_i - \overline{\ln \lambda})^2} \right]^{\frac{1}{2}} \quad (2)$$

where e_i is the error of the Ångström relationship, n is the number of wavelengths λ_i used to fit the Ångström relationship, and $\overline{\ln \lambda}$ is the average of the logarithm of the wavelengths. e_i can be estimated using the relative error of AOD ($\frac{\Delta AOD}{AOD}$), and the uncertainty of AERONET AOD (ΔAOD) is considered as 0.01 here. According to Eq. 2, the uncertainty of AE is roughly inversely proportional to AOD, with larger errors at lower AOD conditions. Li et al. (2014) evaluated that the uncertainty of $AE_{440,870}$ was 0.33 when $AOD_{440} = 0.15$, and the uncertainty would rapidly increase to 0.56 when AOD_{440} decreased to 0.08. Eck et al. (1999) also demonstrated significant variability in $AE_{440,870}$ for lower AOD, largely attributed to increased relative errors in AOD at these low values. These results correspond to the inverse relationship between ΔAE and AOD. Therefore, it should be noted that $AE_{440,870}$ is highly uncertain and the $AE_{440,870}$ trends are less robust for sites with low AOD, even if the trends are statistically significant.

Significant negative $AE_{440,870}$ trends are universally found for stations across Europe, the Mediterranean, eastern North America, the Arabian Peninsula, and Middle Asia (Fig. 5, Fig. 6). In contrast, stations in western North America, North India, East Asia, and Southeast Asia mainly exhibit positive $AE_{440,870}$ trends. The negative $AE_{440,870}$ trends for Europe, the Mediterranean, and eastern North America are likely due to reductions in fine-mode anthropogenic aerosol and precursor emissions. In North India, considering the seasonal cycle of $AE_{440,870}$ value (Fig. 6c,d), the positive $AE_{440,870}$ trends for Kanpur and Gandhi_College primarily result from increased fine-mode anthropogenic emissions as well as decreased coarse-mode dust loading. These shifts in anthropogenic emissions have been assessed through satellite observations and emission inventories (Pouliot et al., 2015; Szymankiewicz et al., 2021; Krotkov et al., 2016; Zhao et al., 2017; de Meij et al., 2012; Kumar et al.,

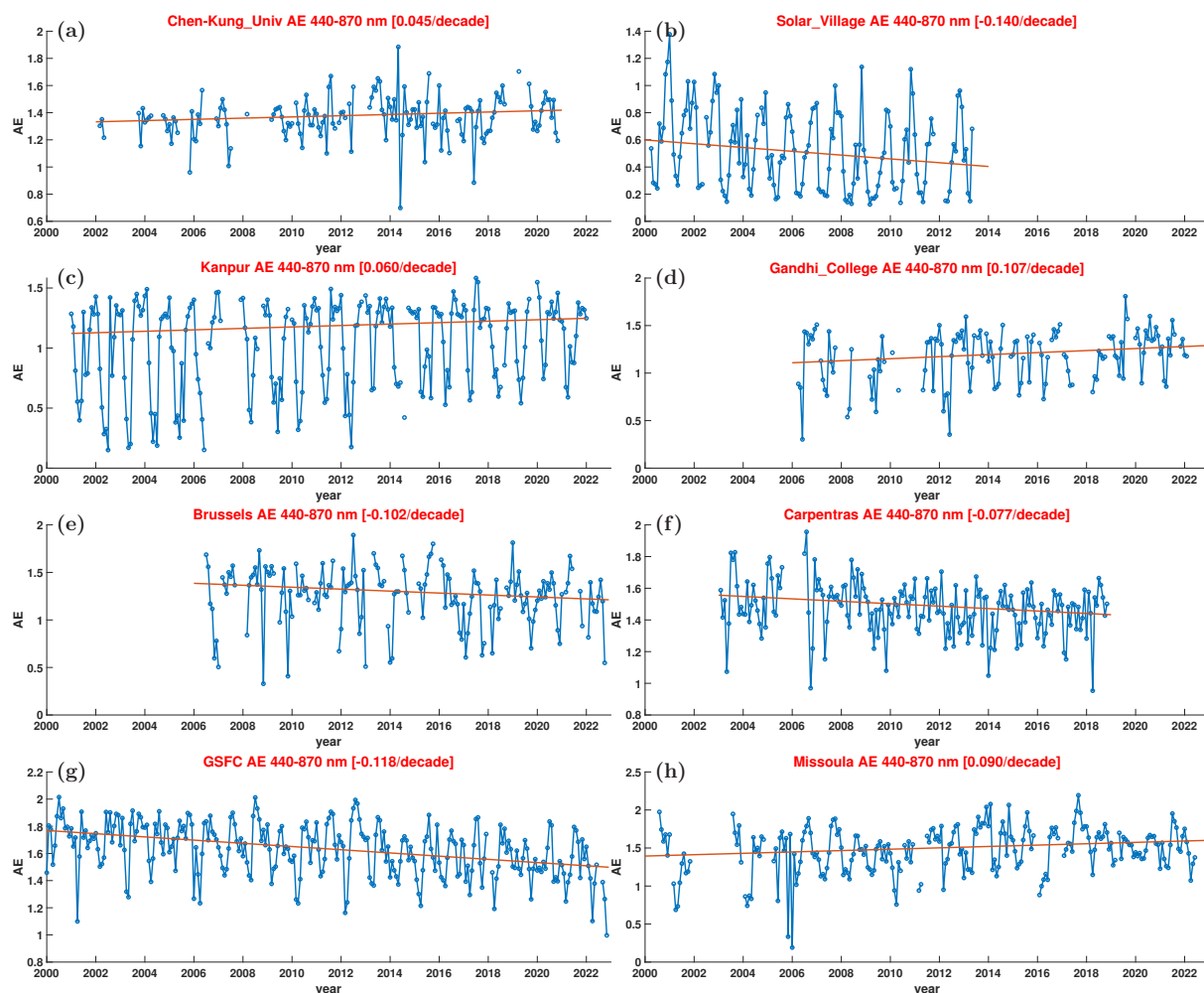


Figure 6. Time series of AE at several representative AERONET stations with trends at 95% significance. (a) Chen-Kung_Univ, (b) Solar_Village, (c) Kanpur, (d) Gandhi_College, (e) Brussels, (f) Carpentras, (g) GSFC, (h) Missoula.

2021), and the decline of dust loading over South Asia was also verified by satellite observations and AERONET measurements (Pandey et al., 2016, 2017; Ramachandran and Rupakheti, 2022; Kaskaoutis et al., 2011). The Arabian Peninsula is a well-known dust source (Ginoux et al., 2012) and the $AE_{440,870}$ values are typically low (Fig. 6b), therefore the negative $AE_{440,870}$ trend for Solar_Village is likely attributed to increased dust activities. Conversely, the increased $AE_{440,870}$ in western North America might be partly due to both increases in biomass burning aerosols and possibly diminished dust sources. These inferences align with previous studies, as Shao et al. (2013) also reported positive dust trends in the Middle East and negative trends in North America, whereas Eck et al. (2023) and Iglesias et al. (2022) revealed increases in biomass burning emissions over western North America. Over Asia, significant positive $AE_{440,870}$ trends are predominantly observed in the Korean Peninsula, the Indochina Peninsula, and the Taiwan Island, which might be linked to decreases in coarse-mode aerosols,

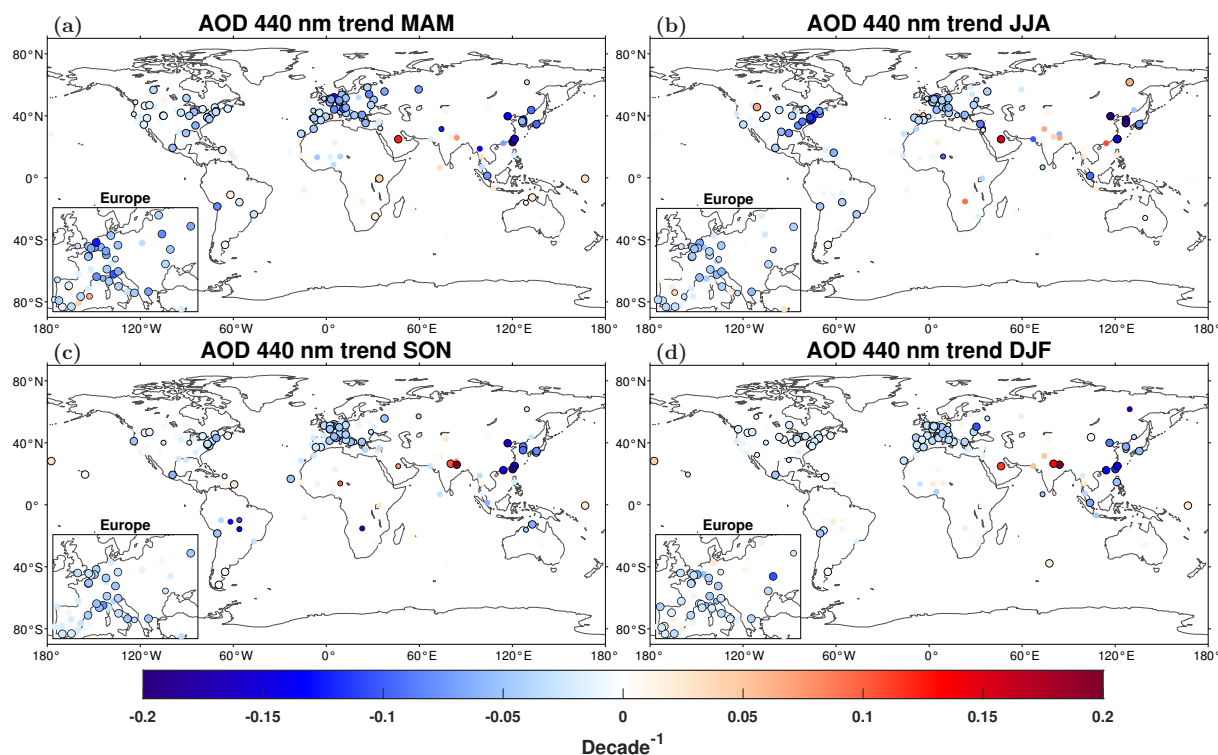


Figure 7. Seasonal trends of 440 nm AOD at AERONET stations. Dots without black boundary indicate trends below 90% significance level. Smaller dots with black boundary indicate trends at 90% significance, and larger dots with black boundary indicate trends at 95% significance. The magnitude of the trend has the unit of [per decade].

195 such as the observed decline of dust transported from the mainland (Zhang et al., 2021; Kim et al., 2017; Cho et al., 2021), and is consistent with the decline in dust emissions in the mainland reported by previous studies (Wang et al., 2021a; Wu et al., 2022; Wang et al., 2021b; Zhao et al., 2018). Notably, Beijing, Xianghe, and Hong_Kong_PolyU, despite showing substantial AOD_{440} reductions, exhibit no significant $AE_{440-870}$ trends, which might be related to reductions in both anthropogenic fine-mode aerosols and coarse-mode dust in these areas.

200 The spatial distribution of seasonal AOD_{440} (Fig. 7) and $AE_{440-870}$ (Fig. 8) trends is generally similar to that of annual results. Nevertheless, the magnitude of the trends could vary by season, and certain stations might exhibit significant trends only during particular seasons. This variation is largely attributed to the seasonal patterns of aerosol emissions and meteorological conditions. For example, in Europe and North America, a greater number of stations exhibit significant AOD_{440} trends in MAM (Fig. 7a), while $AE_{440-870}$ trends in DJF (Fig. 8d) are more pronounced and deviate more from the annual results. This is because aerosol concentrations are typically higher in spring and lower in winter in the Northern Hemisphere (Fig. 4), allowing for more substantial reductions in spring and more significant compositional variations in winter. However, $AE_{440-870}$ trends at low AOD seasons, such as the more pronounced $AE_{440-870}$ trends in winter in the Northern Hemisphere, should be treated

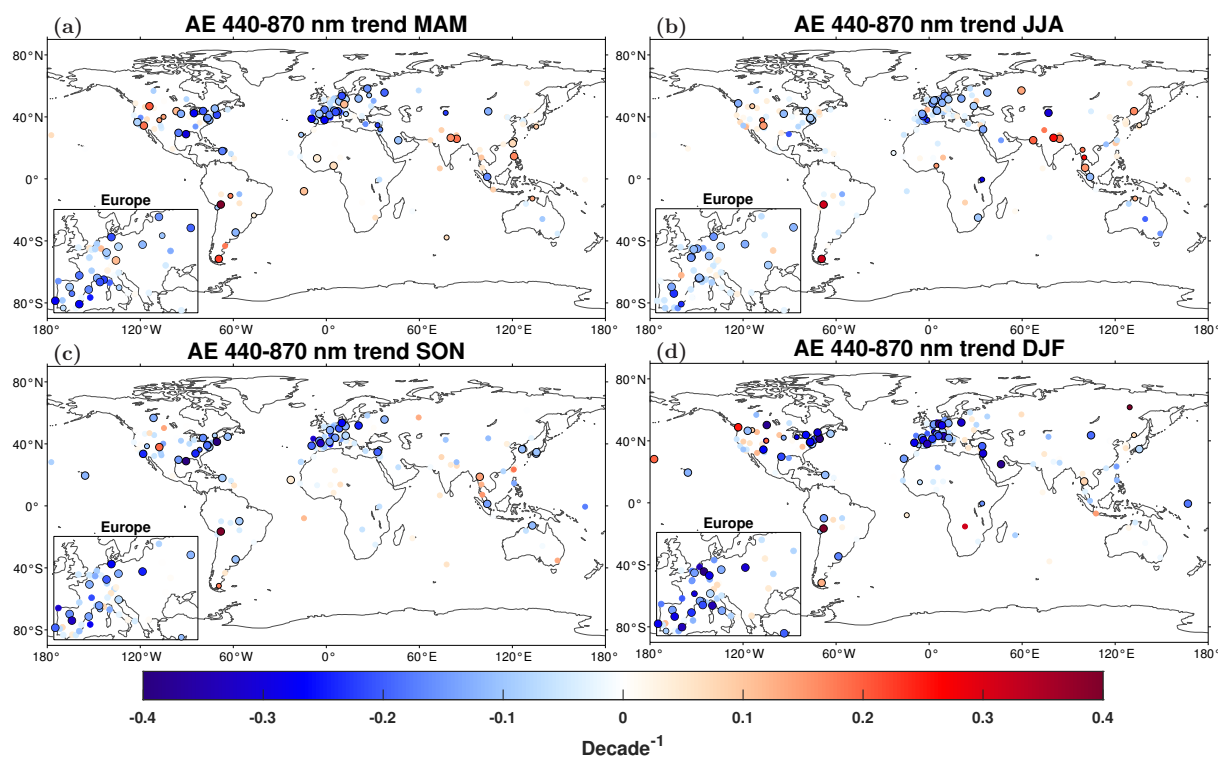


Figure 8. Same as Fig. 7, but with trends of AE.

with caution, because the uncertainty in $AE_{440,870}$ becomes large at low AOD conditions. In North India, Gandhi_College and Kanpur only exhibit significant AOD_{440} trends in SON (Fig. 7c) and DJF (Fig. 7d), while significant $AE_{440,870}$ trends
 210 predominantly occur in MAM (Fig. 8a) and JJA (Fig. 8b). We can find that $AE_{440,870}$ values at these stations in North India significantly exceed 1.0 in SON and DJF (Fig. 6c,d), suggesting the predominance of fine-mode anthropogenic aerosols in these seasons. In contrast, $AE_{440,870}$ values in MAM and JJA start at approximately 0.5, emphasizing the dominance of coarse-mode aerosols, and rise to about 1.0 in recent years, suggesting a largely increased fraction of fine-mode aerosols. The seasonal patterns of AOD and AE in South Asia have also been verified through multi-year observations (Adhikary et al.,
 215 2007; Kaskaoutis et al., 2012). During the pre-monsoon (March-May) and monsoon (June-September) seasons, higher wind speeds and stronger precipitation lead to stronger dust activities and higher wet scavenging of aerosols, whereas in the post-monsoon (October-November) and winter (December-February) the meteorological conditions become reversed, with weaker dust activities and less efficient wet removal of aerosols occurred (Moorthy and Babu, 2006; Henriksson et al., 2011). As a result, in SON and DJF, the rises in anthropogenic emissions, mainly crop residue burning in post-monsoon and biofuel and
 220 fossil fuel burning in winter (Yin, 2020; Bhardwaj et al., 2015; Venkataraman et al., 2018), have a negligible impact on changes in aerosol compositions and $AE_{440,870}$ values, but would lead to the significant positive AOD_{440} trends under less efficient wet removal. On the other hand, in MAM and JJA, stronger wet scavenging of aerosols makes the AOD trend less pronounced, and

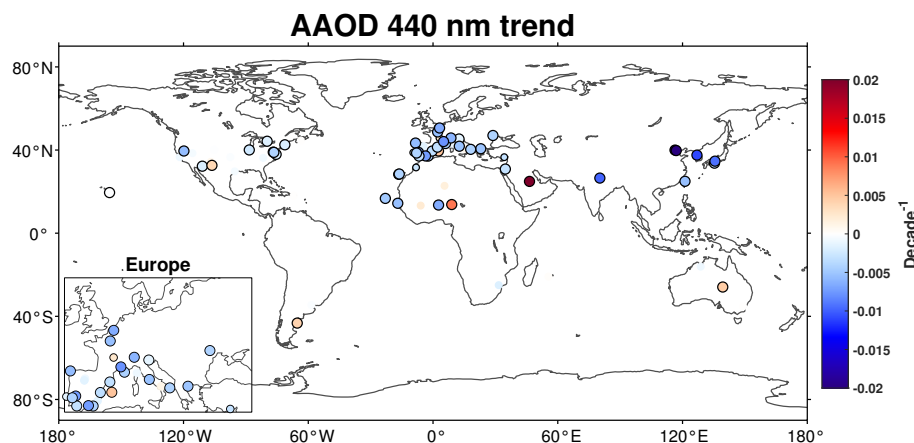


Figure 9. Same as Fig. 3, but with trends of AAOD.

the dominant aerosol type, dust, is mainly affected by natural variability (Kaskaoutis et al., 2012) and exhibits a negative trend (Pandey et al., 2017; Ramachandran and Rupakheti, 2022). Therefore, the increase in anthropogenic aerosols, i.e., biomass and biofuel burning emissions, fossil fuel emissions, and industry emissions (Venkataraman et al., 2018; Ramachandran and Rupakheti, 2022), does not have a significant impact on the total AOD₄₄₀ in these two seasons, but serves to increase the fine mode fractions, leading to the insignificant AOD₄₄₀ trends and significant positive AE_{440_870} trends.

3.2 Trends for AAOD and SSA

AAOD and SSA both characterize the scattering and absorption properties of aerosols. AAOD represents the total aerosol absorption optical depth, whereas SSA reflects the relative contribution of scattering to total extinction. Therefore, the AAOD trend directly reflects changes in the amount of absorbing aerosols, while the SSA trend is related to variations of both absorbing and scattering aerosols. The relationship between the two parameters can be expressed as the following equation:

$$\text{AAOD} = (1 - \text{SSA}) \times \text{AOD} \quad (3)$$

Before presenting the trends, it is important to acknowledge the uncertainties associated with AERONET inversion parameters. AERONET implements a series of quality control criteria for Level 2.0 inversion products. Under these controls, AERONET SSA have an error of ± 0.03 when AOD₄₄₀ ~ 0.4 , and the error is even larger at lower AODs, i.e., an error of ± 0.05 when AOD₄₄₀ ~ 0.2 , and of ± 0.07 when AOD₄₄₀ ~ 0.1 (Sinyuk et al., 2020). As SSA typically varies from approximately 0.8 to 1.0 (Dubovik et al., 2002; Giles et al., 2012), this error is remarkable when examining the variation of SSA and AAOD, i.e. a 0.03 error would lead to a 15% uncertainty. Therefore, the great uncertainties of these parameters should be kept in mind when analyzing trends in this section, especially for regions with low aerosol loadings.

Similar to AOD₄₄₀, significant negative AAOD₄₄₀ trends (Fig. 9, Fig. 10) are universally found for AERONET stations in the Northern Hemisphere, especially in East Asia, North India, Europe and North America, indicating reductions in absorbing

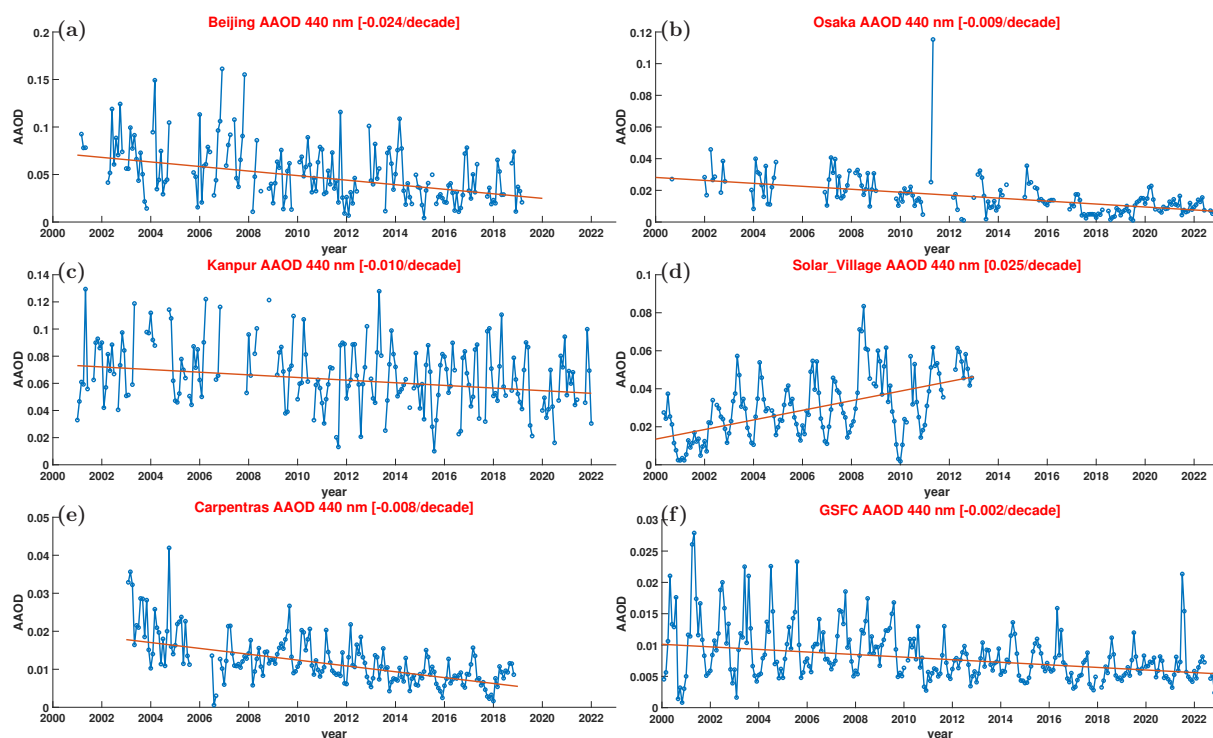


Figure 10. Time series of 440 nm AAOD at several representative AERONET stations with trends at 95% significance. (a) Beijing, (b) Osaka, (c) Kanpur, (d) Solar_Village, (e) Carpentras, (f) GSFC.

species, mainly primary aerosols. Conversely, significant positive AAOD₄₄₀ trend is mainly found for Solar_Village in the Arabian Peninsula (Fig. 10d), suggesting increases in absorbing aerosols. Birdsville in Australia and Trelew in southern South America also exhibit significant positive AAOD₄₄₀ trends, but the magnitude is very low and the results are relatively uncertain because the AAOD₄₄₀ are quite small in these sites. The reductions in AAOD₄₄₀ over East Asia, Europe, North India, and North America are primarily attributed to declines in anthropogenic emissions, such as reduced black carbon (BC) and/or organic carbon (OC) emissions from fossil fuels (Ramachandran and Rupakheti, 2022; He et al., 2023; Li et al., 2024), because aerosols in these regions are mainly of the Urban/Industrial type (Li et al., 2016). Decreased dust emissions discussed in the previous section might also be a potential contributor to the negative AAOD₄₄₀ trends in East Asia, North India, and western North America (Shao et al., 2013; Zhang et al., 2019; Wang et al., 2021b; Ramachandran and Rupakheti, 2022; Pandey et al., 2017), but the effect might not be as substantial as that of anthropogenic emissions, since dust is not the dominant type in these regions. Significant positive AAOD₄₄₀ trend for Solar_Village in the Arabian Peninsula is likely attributed to increased dust loading. As dust mainly exhibits strong absorption for short wavelengths, AAOD trends at other channels with longer wavelengths might not be that significant.

The SSA₄₄₀ trends (Fig. 11, Fig. 12) are generally opposite to the AAOD₄₄₀ trends, with exceptions in some stations in central Europe and North America. The majority of stations in North India, East Asia, and Europe, which also have negative

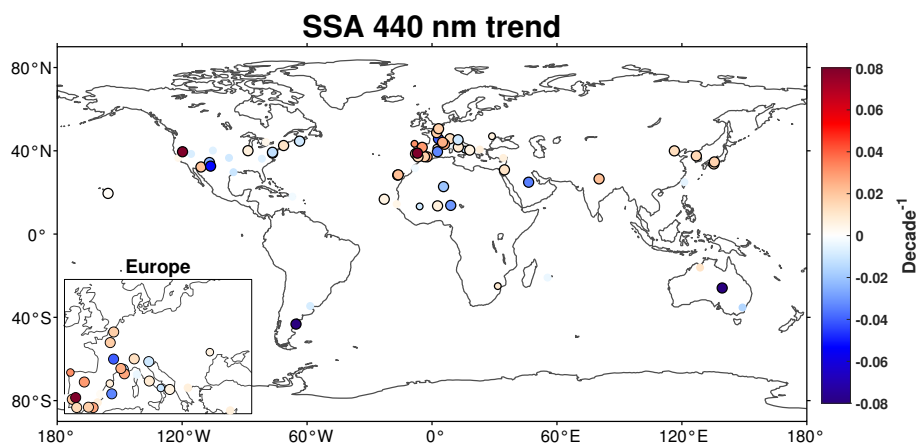


Figure 11. Same as Fig. 3, but with trends of SSA.

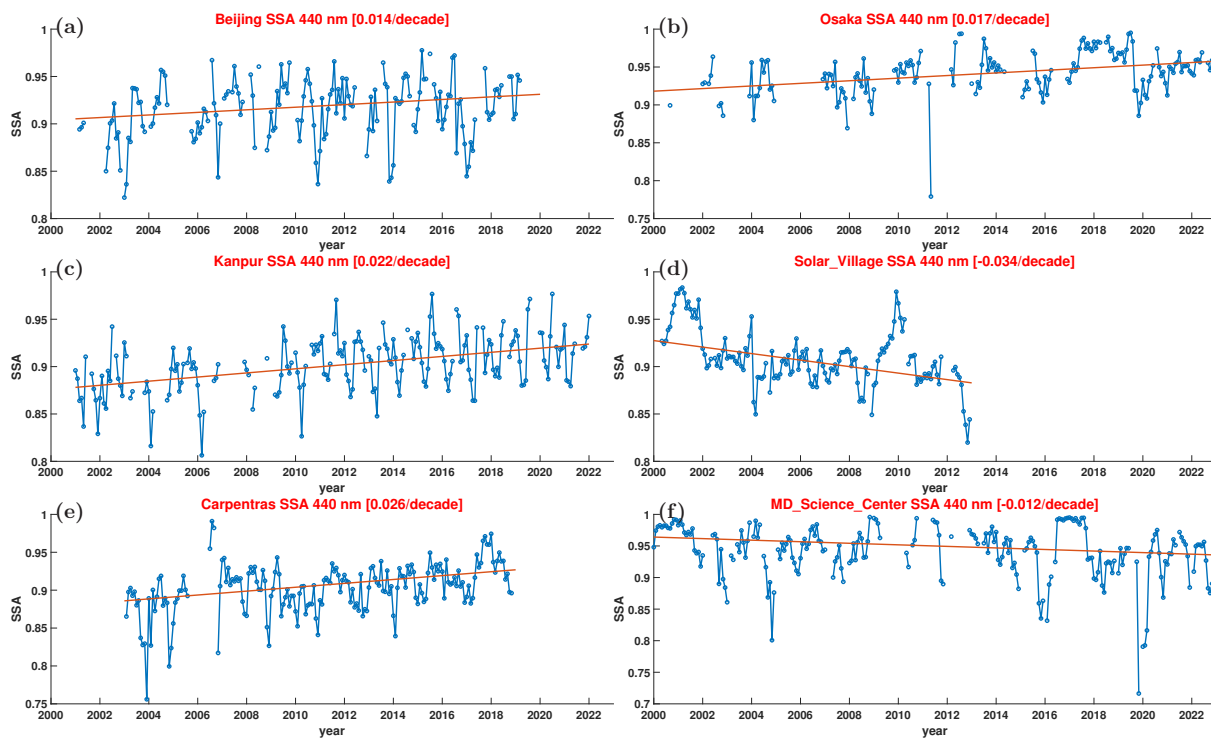


Figure 12. Time series of 440 nm SSA at several representative AERONET stations with trends at 95% significance. (a) Beijing, (b) Osaka, (c) Kanpur, (d) Solar_Village, (e) Carpentras, (f) MD_Science_Center.

AAOD₄₄₀ trends, exhibit significant positive SSA₄₄₀ trends, corresponding to a decrease in the fraction of absorbing aerosols over time. Remember that a rise in total aerosol loading is found for North India (Fig. 3), indicating a more pronounced in-

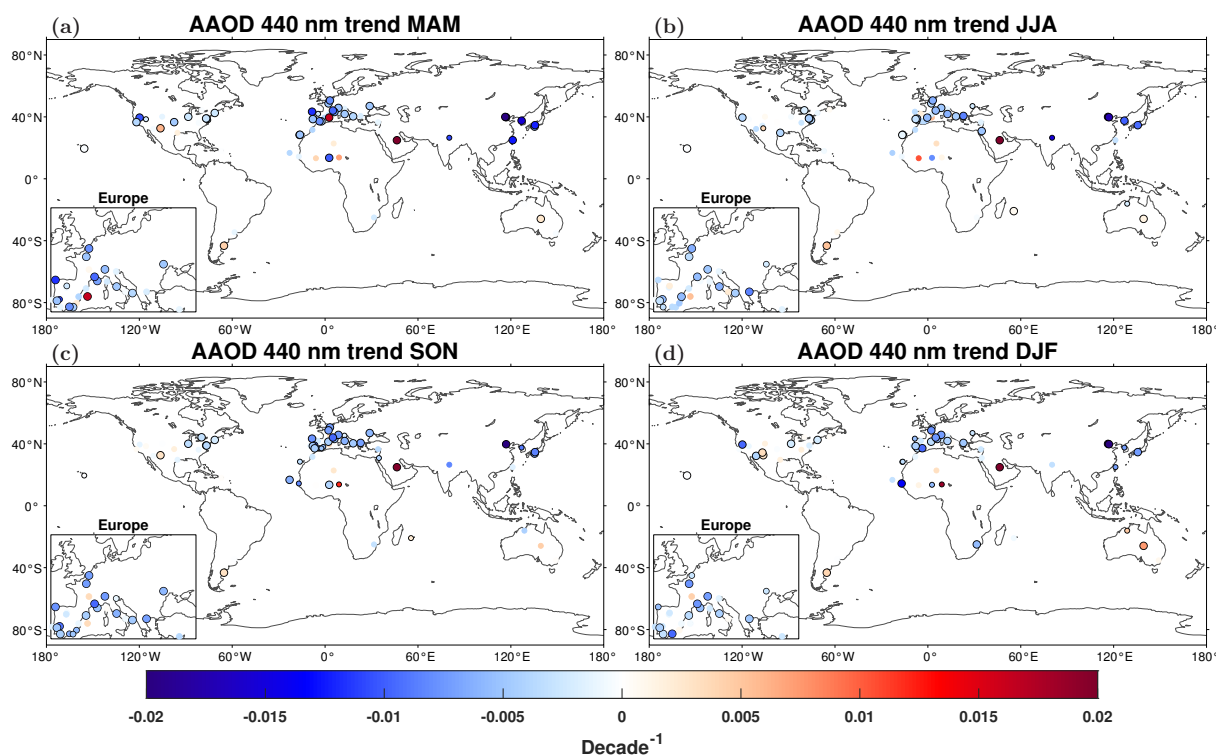


Figure 13. Same as Fig. 7, but with trends of AAOD.

crease in scattering aerosols, such as sulfates, than the decrease in absorbing species. For East Asia and Europe, the decreases in AOD_{440} (Fig. 3) and $AAOD_{440}$ (Fig. 9) demonstrate possible reductions in both scattering and absorbing aerosols, while positive SSA_{440} trends further suggest stronger reductions in absorbing species in these regions. Four stations in central Europe exhibit significant negative SSA_{440} trends. SSA_{440} trends show large spatial heterogeneity in North America, with five stations exhibiting significant positive trends, four with significant negative trends, and four with weak negative trends not reaching the 90% significance threshold. Stations with decreased SSA_{440} over central Europe and North America exhibit only a mild decrease or even a slight increase in $AAOD_{440}$ (Fig. 9, Fig. 10f), implying that AOD_{440} reduction in these regions is mainly attributed to scattering aerosols such as sulfates, thereby increasing the proportion of absorbing aerosols. This result aligns with Collaud Coen et al. (2020), which also found SSA reductions in central Europe and North America through in situ measurements, and attributed them to significant decreases in primarily scattering secondary aerosols. The substantial reductions in precursors of these scattering aerosols were also confirmed by satellite observations and emission inventories (Szymankiewicz et al., 2021; Fioletov et al., 2023; Krotkov et al., 2016; Tong et al., 2015). Positive SSA_{440} trend for Solar_Village (Fig. 12d) in the Arabian Peninsula is attributed to increases in absorbing dust aerosols.

Seasonally, although some stations, mainly in North America and Europe, exhibit significant trends primarily during particular seasons, the spatial patterns of seasonal $AAOD_{440}$ (Fig. 13) and SSA_{440} (Fig. 14) trends are overall similar to those

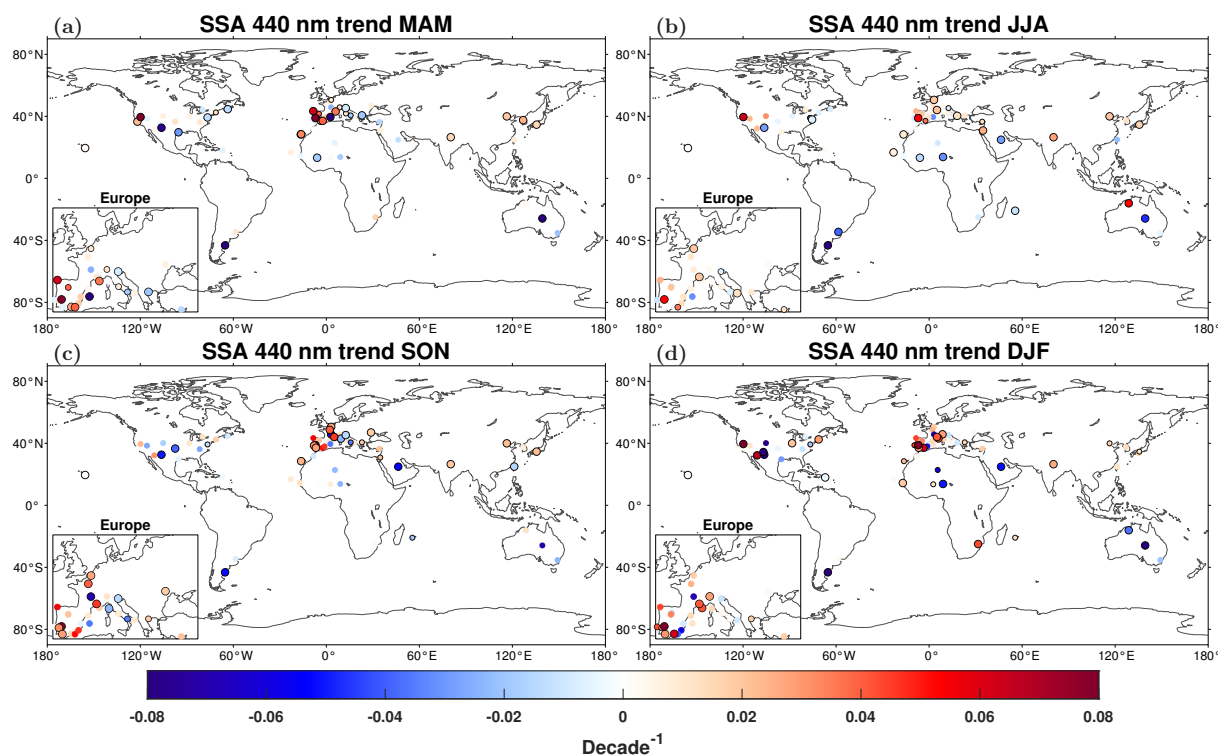


Figure 14. Same as Fig. 7, but with trends of SSA.

275 of annual trends. It is notable that Kanpur in North India exhibits stronger and more significant negative AAOD_{440} trends in MAM (Fig. 13a) and JJA (Fig. 13b) where dust is the dominant aerosol type, further verifying that the decreased AAOD_{440} is partly attributed to the decline in dust loading. As for SSA_{440} , the positive trends for Kanpur are significant at all the four seasons, indicating that the increased anthropogenic emissions in North India are mainly scattering species.

3.3 Aerosol type changes

280 To better explain the aerosol parameter changes, we make a further attempt to classify the measurements into six aerosol types as described in Sect. 2.3, and examine the long-term changes of the loadings for each type. The global AOD_{440} trends of the six aerosol types are shown in Fig. 15.

Significant positive trend for dust AOD is found for Solar_Village, suggesting increased dust activities over the Arabian Peninsula, which is consistent with analysis in previous sections and other studies using satellite observations and AERONET
285 measurements (Mehta et al., 2016; Habib et al., 2019; Sabetghadam et al., 2021; Al Otaibi et al., 2019; Li et al., 2014). We do not find significant trends over other dust sources, as dust loading can have strong decadal variability which often does not yield monotonic trends. Dust trend can also be difficult to detect when combined with fine mode anthropogenic aerosols. The Mixture type straddles the boundary between Dust type and fine-mode types and is affected by both coarse-mode and fine-

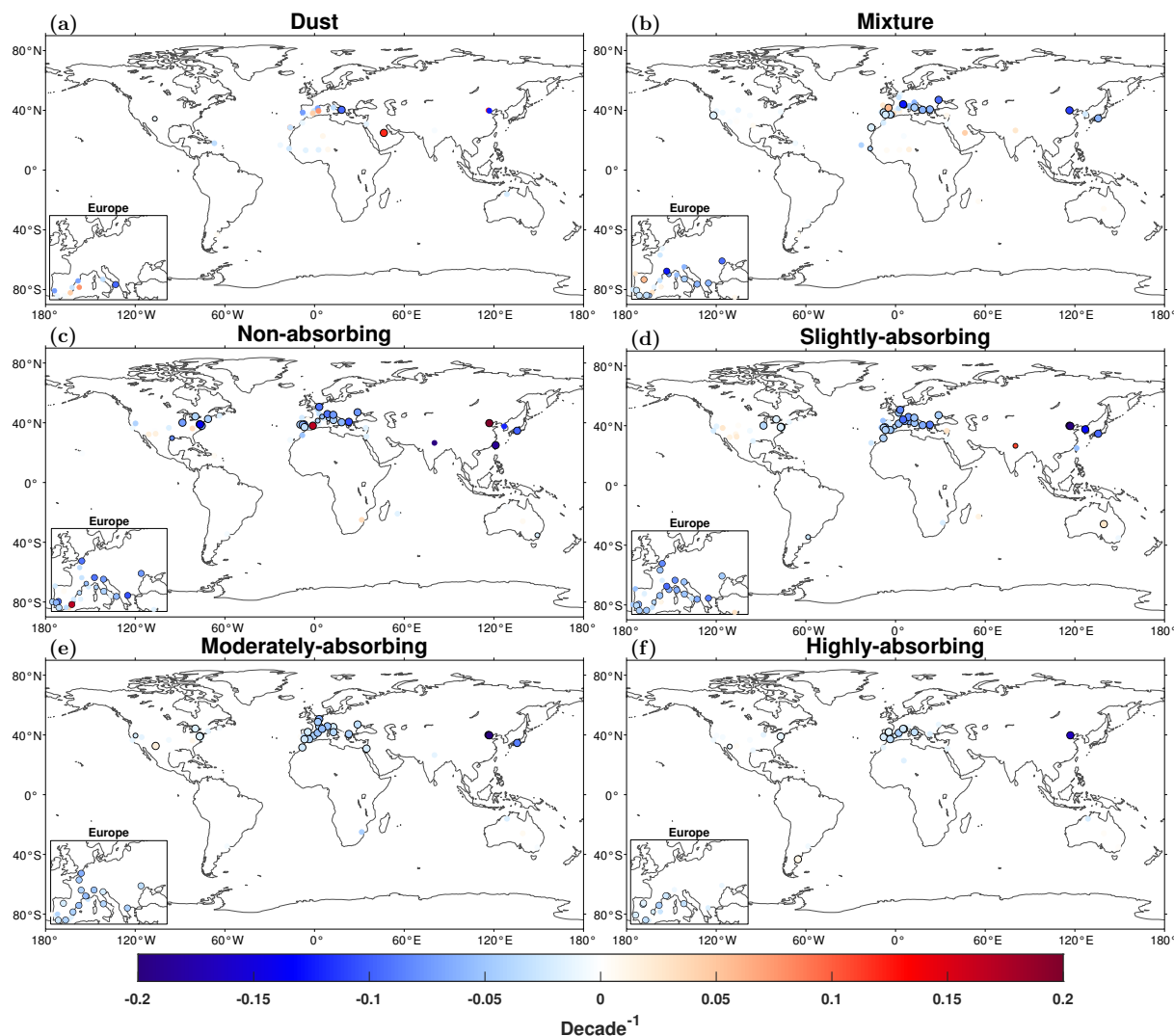


Figure 15. Same as Fig. 3, but with trends of AOD for 6 aerosol types. (a) dust, (b) Mixture, (c) Non-absorbing Fine, (d) Slightly-absorbing Fine, (e) Moderately-absorbing Fine, (f) Highly-absorbing Fine.

mode particles. Significant negative AOD trends in the Mixture type are mainly found over East Asia and Europe (Fig. 15b).
 290 Since East Asia and Europe are both predominated by fine-mode aerosols (Li et al., 2016; Zhang and Li, 2019), the decreased
 Mixture aerosols are thus primarily due to reductions in fine-mode anthropogenic emissions.

The majority of stations in Europe, North America, and East Asia exhibit significant negative AOD trends in four fine-mode
 types (Fig. 15c-f), corresponding to the reduction in both absorbing and scattering anthropogenic emissions revealed by the
 reductions in AOD (Fig. 3) and AAOD (Fig. 9) in these regions. The great reduction in absorbing types (SA, MA and HA) is
 295 also the possible reason for the increase of SSA (Fig. 11). It is notable that Xianghe in East Asia exhibits a significant positive



trend in non-absorbing type (NA) and even larger negative trends in the absorbing types, suggesting a great reduction in BC and/or OC emissions which might potentially lead to a shift in the predominance of aerosol type in pollution events (Zhang and Li, 2019). Eastern North America exhibits a greater reduction in non-absorbing aerosols than that in absorbing species, thus lead to an decrease in SSA (Fig. 11). Kanpur in North India exhibits significant positive trends on SA aerosols, and does not exhibit significant trends on other types. Compared to MA and HA, the SA type is more scattering with lower BC proportion. As fine mode aerosols in Kanpur are initially absorbing types (Pandey et al., 2016), the increase in SA loading suggests a decreased proportion of BC, making the fine mode aerosols in this region more scattering.

4 Discussion and Conclusion

In this study, we investigate trends in aerosol optical parameters using AERONET measurements. Globally, a universal decrease in AOD and AAOD, along with an increase in SSA, is observed at the majority of AERONET stations. The result generally aligns with the previous trend analysis using AERONET Version 2 products ending in 2013 (Li et al., 2014), highlighting the continuity of these trends over time on a global scale. Although our analysis is based on measurements at ground-based stations, coherent spatial patterns over different stations could also indicate regional features, which have also been demonstrated by satellite observations, model simulations, and emission inventories (Gupta et al., 2022; de Meij et al., 2012; Fioletov et al., 2023; Mishchenko et al., 2007; Wei et al., 2021b, a; Yoon et al., 2016). Similar to Li et al. (2014), no significant seasonality is detected in the aerosol parameters examined in this work. Taking advantages of longer records and improved station coverage, this study identifies more detailed regional trends and finds some new spatial patterns.

Spatially, significant negative AOD_{440} trends are universally observed across East Asia and Southeast Asia, which are not demonstrated by Li et al. (2014). This discrepancy indicates that the pronounced decrease in aerosols within these regions primarily occurred over the last decade, which is also supported by satellite observations and model simulations (Fioletov et al., 2023; de Meij et al., 2012; Zhao et al., 2017; Krotkov et al., 2016; Mehta et al., 2016). The most substantial reduction in AOD_{440} occurs in East China, consistent with emission inventories (Kurokawa and Ohara, 2020). Correspondingly, Li et al. (2014) also reported no significant $AE_{440-870}$ trends, while our analysis reveals significant positive $AE_{440-870}$ trends at coastal stations, aligning with in situ measurements (Collaud Coen et al., 2020). The increase in $AE_{440-870}$ implies a reduction in aerosol particle size, potentially due to decreased dust transportation from the mainland. Compared to Li et al. (2014), this study also finds that more stations in mid-latitude East Asia exhibit significant negative $AAOD_{440}$ trends and positive SSA_{440} trends which are mainly attributed to decreased absorbing primary aerosols, in agreement with other independent studies utilizing AERONET data (Ramachandran and Rupakheti, 2022; Ramachandran et al., 2020; Tao et al., 2017; Yu et al., 2022; Eom et al., 2022).

Coherent significant decreases of AOD_{440} and $AAOD_{440}$ found for Europe and North America are consistent with Li et al. (2014), and are in good agreement with satellite observations (Mehta et al., 2016; Zhao et al., 2017; Krotkov et al., 2016; Fioletov et al., 2023) as well as in situ measurements of recent aerosol absorbing and scattering trends (Collaud Coen et al., 2020). These trends support the ongoing efforts in emission control throughout this century. However, while Li et al. (2014)



observed smaller AOD_{440} trends in North America compared to Europe, this study reports similar and weaker trends for both
330 regions. The decrease in anthropogenic emissions in Europe and North America started in the previous century and has led to
a significant reduction in aerosol loading (de Meij et al., 2012; Szymankiewicz et al., 2021; Rafaj et al., 2013), resulting in a
diminished rate of reduction in aerosol and aerosol precursor emissions over the last decade (Krotkov et al., 2016; Fioletov
et al., 2023; Jiang et al., 2018). Consequently, this potentially leads to smaller AOD_{440} and $AAOD_{440}$ trends, alongside a
reduced discrepancy in AOD_{440} trends between the two regions. Additionally, the update to AERONET Version 3 and slight
335 methodological differences in trend evaluation may also explain some inconsistencies in trend slope assessments. The observed
decline in $AE_{440,870}$ and increase in SSA_{440} in Europe are in line with Li et al. (2014), while the positive $AE_{440,870}$ trends
found for the whole North America by Li et al. (2014) are mainly found in western North America in this work, with eastern
North America exhibiting negative trends. This indicates that significant reductions in dust emissions are primarily concentrated
in western North America along with increases in biomass burning emissions, with the impact on eastern areas being less
340 pronounced, consistent with dust monitoring results (Aryal and Evans, 2022) and trends in western North America forest fires
(Eck et al., 2023; Iglesias et al., 2022). The SSA_{440} trends in this work also diverge from the coherent positive trends reported
by Li et al. (2014), because we find negative SSA_{440} trends for a small proportion of European stations and for more than
half of the North American stations. This discrepancy is likely due to differences in study periods, and the trends observed in
this work align with those from in situ measurements conducted over similar periods (Collaud Coen et al., 2020), suggesting a
345 larger decline in scattering aerosols than absorbing species.

The positive AOD_{440} , $AE_{440,870}$ and SSA_{440} trends for Kanpur in North India identified by Li et al. (2014) are corroborated
in this work, suggesting increased fine-mode anthropogenic aerosol loading. Unlike the report by Li et al. (2014) which found
no significant trend in $AAOD$ for Kanpur, our research reveals a significant negative $AAOD_{440}$ trend, indicating recent de-
creases in absorbing aerosols in the region, and we further attribute this change to both decreased anthropogenic BC emissions
350 and decreased dust loading according to seasonal trend analysis and type analysis, consistent with previous studies (Pandey
et al., 2016, 2017; Ramachandran and Rupakheti, 2022). The trends over North India exhibit strong seasonality, with signif-
icant positive AOD_{440} trends in SON and DJF where anthropogenic aerosols are predominant, and decreased $AAOD_{440}$ and
increased $AE_{440,870}$ in MAM and JJA where dust loading is stronger, suggesting that these seasonal trends may be associated
with the seasonal cycle of aerosol emissions and meteorological conditions. Furthermore, an additional site, Gandhi_College,
355 located in North India as well, also exhibits significant positive AOD_{440} trends and positive $AE_{440,870}$ trends, highlighting an
increase in fine-mode aerosols across South Asia. The AOD_{440} and $AE_{440,870}$ trends for both Kanpur and Gandhi College,
along with $AAOD_{440}$ and SSA_{440} trends for Kanpur, align with independent studies utilizing AERONET measurements (Ra-
machandran and Rupakheti, 2022; Kumar et al., 2022; Kaskaoutis et al., 2012) and satellite observations (Ramachandran et al.,
2020; Kaskaoutis et al., 2011), further verifying the increment in aerosols and the alteration of aerosol compositions in North
360 India.

The AERONET products for Solar_Village end in 2013, therefore the trends of these aerosol optical parameters are the same
as those reported by Li et al. (2014), with positive AOD_{440} and $AAOD_{440}$ trends, and negative $AE_{440,870}$ and SSA_{440} trends,



which is probably due to the increased dust activities in the Arabian Peninsula, and was also demonstrated in previous studies (Al Otaibi et al., 2019; Habib et al., 2019).

365 As a further step, we classify the aerosol observations into six types using FMF_{550} and SSA_{440} , and examine the changes in aerosol loadings of each type. The trends for different aerosol types further verify the trends of AERONET parameters and offer insights into aerosol composition changes. We only find significant positive dust loading trend in the Arabian Peninsula. Significant trends mainly concentrate on fine-mode types, with declines in both absorbing types and the non-absorbing type globally, consistent with the negative AOD_{440} and $AAOD_{440}$ trends. Spatially, the majority of stations in East Asia and Europe
370 exhibit stronger reductions in absorbing aerosols than those in non-absorbing types, whereas in eastern North America the reduction in AOD_{440} is mainly attributed to non-absorbing species. The results can fully explain the changes in SSA_{440} , which exhibit positive trends over East Asia and Europe and negative trends over eastern North America. Significant positive SA loading trend found in North India suggests a decrease in BC proportion which leads to increased SSA_{440} .

This study provides insights into temporal variations in aerosol loading, optical properties, and aerosol types. Decreases in
375 AOD across Europe, North America, and East Asia reflect the effectiveness of emission control policies implemented in these regions. For instance, there has been a significant reduction in AOD over China in the past decade due to the Air Pollution Prevention and Control Action Plan (Gupta et al., 2022; Zhao et al., 2017). Conversely, the increase of AOD over North India and the Arabian Peninsula indicates deteriorating air quality, posing potential risks to public health. The substantial changes in SSA and $AAOD$ observed in many regions are of concern for climate models due to their critical relationship with aerosol
380 climate effects, potentially influencing regional energy budget, atmospheric circulation, the water cycle, etc. Previous studies have indicated that failure to capture the increase in SSA over northern India in climate models likely contributed to their biases in simulating the negative precipitation trend in this region (Ying et al., 2023). Furthermore, trends in aerosol properties and types are crucial for satellite remote sensing applications, as many algorithms rely on assumed aerosol models clustered from AERONET observations. Updating these models to reflect changes in aerosol types may be necessary (Zhang et al., 2024).

385 It is important to note that our analysis extends through 2022, encompassing the COVID-19 pandemic. Previous studies have documented significant reductions in aerosol loading and notable changes in aerosol compositions due to decreased anthropogenic emissions in regions implementing lockdown policies, such as East Asia, Europe, and North America (Cao et al., 2021; Clemente et al., 2022; Liang et al., 2023; Sokhi et al., 2021). We observed abnormally low AOD values at certain stations during this period, including Xianghe and Chen-Kung_ Univ (Fig. 4a, c). This could potentially lead to a negative bias
390 in AOD trends and contribute to discrepancies with other research on aerosol trends at these stations. However, since this period accounts for only about 10% of our total study period, and many stations lack Level 2.0 records for this time, the impact on trend analysis by COVID-19 is likely minimal at the majority of the stations.

The main purpose of this work is to update the trends in aerosol parameters with larger size of stations and longer records with respect to Li et al. (2014). We do note remarkable changes in aerosol trends over regions such as East Asia and the Southern
395 Hemisphere, whereas patterns in other regions remain relatively stable. Most additional stations in this study are located in Europe and North America, where the distribution of stations is already dense to deduce general features of aerosol trends in these regions. We still lack insights into aerosol trends across other regions, including Asia, Africa, South America, Australia,



and polar and oceanic regions where the spatial coverage of stations is insufficient, and some stations such as Solar_Village do not have Level 2.0 data in recent years. There is still need to establish more stations in Asia and the Southern Hemisphere to
400 better capture the rapid change of aerosol properties there.

Author contributions. JL designed the research. TE, PG, BH, OD, and EL gathered the datasets and applied additional QAC to the data. ZZ selected the stations with long-term records, computed the trends, and analyzed the results. ZZ and JL prepared the manuscript draft. YD, TE, PG, SNT, and JK reviewed and edited the manuscript. All the other co-authors contributed to the measurements of aerosol optical properties applied in this work and to the manuscript review.

405 *Competing interests.* The authors declare that they have no conflict of interest.

Acknowledgements. We gratefully thank the AERONET team, especially the PIs and Co-Is and their staff of the 165 selected stations, for establishing and maintaining the sites and providing the data used in this study. The AERONET data are obtained from the AERONET website, <https://aeronet.gsfc.nasa.gov/>. This study is funded by the National Key Research and Development Program of China (grant no. 2023YFF0805401) and the National Natural Science Foundation of China (NSFC) Grants Nos. 42175144 and 42375121.



410 References

- Adhikary, B., Carmichael, G. R., Tang, Y., Leung, L. R., Qian, Y., Schauer, J. J., Stone, E. A., Ramanathan, V., and Ramana, M. V.: Characterization of the seasonal cycle of south Asian aerosols: A regional-scale modeling analysis, *Journal of Geophysical Research: Atmospheres*, 112, <https://doi.org/10.1029/2006jd008143>, 2007.
- Al Otaibi, M., Farahat, A., Tawabini, B., Omar, M. H., Ramadan, E., Abuelgasim, A., and P. Singh, R.: Long-Term Aerosol Trends and Variability over Central Saudi Arabia Using Optical Characteristics from Solar Village AERONET Measurements, *Atmosphere*, 10, 752, <https://doi.org/10.3390/atmos10120752>, 2019.
- Aryal, Y. and Evans, S.: Decreasing Trends in the Western US Dust Intensity With Rareness of Heavy Dust Events, *Journal of Geophysical Research: Atmospheres*, 127, <https://doi.org/10.1029/2021jd036163>, 2022.
- Bhardwaj, P., Naja, M., Kumar, R., and Chandola, H. C.: Seasonal, interannual, and long-term variabilities in biomass burning activity over South Asia, *Environmental Science and Pollution Research*, 23, 4397–4410, <https://doi.org/10.1007/s11356-015-5629-6>, 2015.
- Cao, Y., Shao, L., Jones, T., Oliveira, M. L., Ge, S., Feng, X., Silva, L. F., and Bérubé, K.: Multiple relationships between aerosol and COVID-19: A framework for global studies, *Gondwana Research*, 93, 243–251, <https://doi.org/10.1016/j.gr.2021.02.002>, 2021.
- Cho, J. H., Kim, H. S., and Chung, Y. S.: Spatio-temporal changes of PM10 trends in South Korea caused by East Asian atmospheric variability, *Air Quality, Atmosphere & Health*, 14, 1001–1016, <https://doi.org/10.1007/s11869-021-00995-y>, 2021.
- Clemente, A., Yubero, E., Nicolás, J. F., Caballero, S., Crespo, J., and Galindo, N.: Changes in the concentration and composition of urban aerosols during the COVID-19 lockdown, *Environmental Research*, 203, 111 788, <https://doi.org/10.1016/j.envres.2021.111788>, 2022.
- Collaud Coen, M., Andrews, E., Alastuey, A., Arsov, T. P., Backman, J., Brem, B. T., Bukowiecki, N., Couret, C., Eleftheriadis, K., Flentje, H., Fiebig, M., Gysel-Beer, M., Hand, J. L., Hoffer, A., Hooda, R., Hueglin, C., Joubert, W., Keywood, M., Kim, J. E., Kim, S.-W., Labuschagne, C., Lin, N.-H., Lin, Y., Lund Myhre, C., Luoma, K., Lyamani, H., Marinoni, A., Mayol-Bracero, O. L., Mihalopoulos, N., Pandolfi, M., Prats, N., Prenni, A. J., Putaud, J.-P., Ries, L., Reisen, F., Sellegri, K., Sharma, S., Sheridan, P., Sherman, J. P., Sun, J., Titos, G., Torres, E., Tuch, T., Weller, R., Wiedensohler, A., Zieger, P., and Laj, P.: Multidecadal trend analysis of in situ aerosol radiative properties around the world, *Atmospheric Chemistry and Physics*, 20, 8867–8908, <https://doi.org/10.5194/acp-20-8867-2020>, 2020.
- de Meij, A., Pozzer, A., and Lelieveld, J.: Trend analysis in aerosol optical depths and pollutant emission estimates between 2000 and 2009, *Atmospheric Environment*, 51, 75–85, <https://doi.org/10.1016/j.atmosenv.2012.01.059>, 2012.
- Dubovik, O. and King, M. D.: A flexible inversion algorithm for retrieval of aerosol optical properties from Sun and sky radiance measurements, *Journal of Geophysical Research: Atmospheres*, 105, 20 673–20 696, <https://doi.org/10.1029/2000jd900282>, 2000.
- Dubovik, O., Holben, B., Eck, T. F., Smirnov, A., Kaufman, Y. J., King, M. D., Tanré, D., and Slutsker, I.: Variability of Absorption and Optical Properties of Key Aerosol Types Observed in Worldwide Locations, *Journal of the Atmospheric Sciences*, 59, 590–608, [https://doi.org/10.1175/1520-0469\(2002\)059<0590:voaaop>2.0.co;2](https://doi.org/10.1175/1520-0469(2002)059<0590:voaaop>2.0.co;2), 2002.
- Eck, T. F., Holben, B. N., Reid, J. S., Dubovik, O., Smirnov, A., O'Neill, N. T., Slutsker, I., and Kinne, S.: Wavelength dependence of the optical depth of biomass burning, urban, and desert dust aerosols, *Journal of Geophysical Research: Atmospheres*, 104, 31 333–31 349, <https://doi.org/10.1029/1999jd900923>, 1999.
- Eck, T. F., Holben, B. N., Reid, J. S., Sinyuk, A., Giles, D. M., Arola, A., Slutsker, I., Schafer, J. S., Sorokin, M. G., Smirnov, A., LaRosa, A. D., Kraft, J., Reid, E. A., O'Neill, N. T., Welton, E., and Menendez, A. R.: The extreme forest fires in California/Oregon in 2020: Aerosol optical and physical properties and comparisons of aged versus fresh smoke, *Atmospheric Environment*, 305, 119 798, <https://doi.org/10.1016/j.atmosenv.2023.119798>, 2023.



- Eom, S., Kim, J., Lee, S., Holben, B. N., Eck, T. F., Park, S.-B., and Park, S. S.: Long-term variation of aerosol optical properties associated with aerosol types over East Asia using AERONET and satellite (VIIRS, OMI) data (2012–2019), *Atmospheric Research*, 280, 106 457, <https://doi.org/10.1016/j.atmosres.2022.106457>, 2022.
- 450 Farahat, A., El-Askary, H., Adetokunbo, P., and Fuad, A.-T.: Analysis of aerosol absorption properties and transport over North Africa and the Middle East using AERONET data, *Annales Geophysicae*, 34, 1031–1044, <https://doi.org/10.5194/angeo-34-1031-2016>, 2016.
- Fioletov, V. E., McLinden, C. A., Griffin, D., Abboud, I., Krotkov, N., Leonard, P. J. T., Li, C., Joiner, J., Theys, N., and Carn, S.: Version 2 of the global catalogue of large anthropogenic and volcanic SO₂ sources and emissions derived from satellite measurements, *Earth System Science Data*, 15, 75–93, <https://doi.org/10.5194/essd-15-75-2023>, 2023.
- 455 Giles, D. M., Holben, B. N., Eck, T. F., Sinyuk, A., Smirnov, A., Slutsker, I., Dickerson, R. R., Thompson, A. M., and Schafer, J. S.: An analysis of AERONET aerosol absorption properties and classifications representative of aerosol source regions, *Journal of Geophysical Research: Atmospheres*, 117, D17 203, <https://doi.org/10.1029/2012jd018127>, 2012.
- Giles, D. M., Sinyuk, A., Sorokin, M. G., Schafer, J. S., Smirnov, A., Slutsker, I., Eck, T. F., Holben, B. N., Lewis, J. R., Campbell, J. R., Welton, E. J., Korkin, S. V., and Lyapustin, A. I.: Advancements in the Aerosol Robotic Network (AERONET) Version 3 database – automated near-real-time quality control algorithm with improved cloud screening for Sun photometer aerosol optical depth (AOD) measurements, *Atmospheric Measurement Techniques*, 12, 169–209, <https://doi.org/10.5194/amt-12-169-2019>, 2019.
- 460 Ginoux, P., Prospero, J. M., Gill, T. E., Hsu, N. C., and Zhao, M.: Global-scale attribution of anthropogenic and natural dust sources and their emission rates based on MODIS Deep Blue aerosol products, *Reviews of Geophysics*, 50, <https://doi.org/10.1029/2012rg000388>, 2012.
- Gupta, G., Venkat Ratnam, M., Madhavan, B., and Narayanamurthy, C.: Long-term trends in Aerosol Optical Depth obtained across the globe using multi-satellite measurements, *Atmospheric Environment*, 273, 118 953, <https://doi.org/10.1016/j.atmosenv.2022.118953>, 2022.
- 465 Habib, A., Chen, B., Khalid, B., Tan, S., Che, H., Mahmood, T., Shi, G., and Butt, M. T.: Estimation and inter-comparison of dust aerosols based on MODIS, MISR and AERONET retrievals over Asian desert regions, *Journal of Environmental Sciences*, 76, 154–166, <https://doi.org/10.1016/j.jes.2018.04.019>, 2019.
- Hansen, J., Sato, M., and Ruedy, R.: Radiative forcing and climate response, *Journal of Geophysical Research: Atmospheres*, 102, 6831–6864, <https://doi.org/10.1029/96jd03436>, 1997.
- 470 He, C., Niu, X., Ye, Z., Wu, Q., Liu, L., Zhao, Y., Ni, J., Li, B., and Jin, J.: Black carbon pollution in China from 2001 to 2019: Patterns, trends, and drivers, *Environmental Pollution*, 324, 121 381, <https://doi.org/10.1016/j.envpol.2023.121381>, 2023.
- Henriksson, S. V., Laaksonen, A., Kerminen, V.-M., Räisänen, P., Järvinen, H., Sundström, A.-M., and de Leeuw, G.: Spatial distributions and seasonal cycles of aerosols in India and China seen in global climate-aerosol model, *Atmospheric Chemistry and Physics*, 11, 7975–7990, <https://doi.org/10.5194/acp-11-7975-2011>, 2011.
- 475 Holben, B. N., Eck, T. F., Slutsker, I., Tanré, D., Buis, J. P., Setzer, A., Vermote, E., Reagan, J. A., Kaufman, Y. J., Nakajima, T., Lavenu, F., Jankowiak, I., and Smirnov, A.: AERONET—A Federated Instrument Network and Data Archive for Aerosol Characterization, *Remote Sensing of Environment*, 66, 1–16, [https://doi.org/10.1016/S0034-4257\(98\)00031-5](https://doi.org/10.1016/S0034-4257(98)00031-5), 1998.
- Holben, B. N., Eck, T. F., Slutsker, I., Smirnov, A., Sinyuk, A., Schafer, J., Giles, D., and Dubovik, O.: Aeronet’s Version 2.0 quality assurance criteria, in: *Remote Sensing of the Atmosphere and Clouds*, edited by Tsay, S.-C., Nakajima, T., Singh, R. P., and Sridharan, R., SPIE, ISSN 0277-786X, <https://doi.org/10.1117/12.706524>, 2006.
- 480 Hsu, N. C., Gautam, R., Sayer, A. M., Bettenhausen, C., Li, C., Jeong, M. J., Tsay, S.-C., and Holben, B. N.: Global and regional trends of aerosol optical depth over land and ocean using SeaWiFS measurements from 1997 to 2010, *Atmospheric Chemistry and Physics*, 12, 8037–8053, <https://doi.org/10.5194/acp-12-8037-2012>, 2012.



- 485 Iglesias, V., Balch, J. K., and Travis, W. R.: U.S. fires became larger, more frequent, and more widespread in the 2000s, *Science Advances*, 8, <https://doi.org/10.1126/sciadv.abc0020>, 2022.
- Jiang, Z., McDonald, B. C., Worden, H., Worden, J. R., Miyazaki, K., Qu, Z., Henze, D. K., Jones, D. B. A., Arellano, A. F., Fischer, E. V., Zhu, L., and Boersma, K. F.: Unexpected slowdown of US pollutant emission reduction in the past decade, *Proceedings of the National Academy of Sciences*, 115, 5099–5104, <https://doi.org/10.1073/pnas.1801191115>, 2018.
- 490 Kaskaoutis, D. G., Kharol, S. K., Sinha, P. R., Singh, R. P., Badarinath, K. V. S., Mehdi, W., and Sharma, M.: Contrasting aerosol trends over South Asia during the last decade based on MODIS observations, <https://doi.org/10.5194/amtd-4-5275-2011>, 2011.
- Kaskaoutis, D. G., Singh, R. P., Gautam, R., Sharma, M., Kosmopoulos, P. G., and Tripathi, S. N.: Variability and trends of aerosol properties over Kanpur, northern India using AERONET data (2001–10), *Environmental Research Letters*, 7, 024003, <https://doi.org/10.1088/1748-9326/7/2/024003>, 2012.
- 495 Kato, S., Bergin, M. H., Ackerman, T. P., Charlock, T. P., Clothiaux, E. E., Ferrare, R. A., Halthore, R. N., Laulainen, N., Mace, G. G., Michalsky, J., and Turner, D. D.: A comparison of the aerosol thickness derived from ground-based and airborne measurements, *Journal of Geophysical Research: Atmospheres*, 105, 14 701–14 717, <https://doi.org/10.1029/2000jd900013>, 2000.
- Kendall, M. G.: Rank correlation methods, Griffin, London [u.a.], 4. ed., 2. impr. edn., ISBN 0852641990, 1975.
- Kim, H. S., Chung, Y. S., and Cho, J. H.: Long-term variations of dust storms and associated dustfall and related climate factors in Korea during 1997–2016, *Air Quality, Atmosphere & Health*, 10, 1269–1280, <https://doi.org/10.1007/s11869-017-0513-9>, 2017.
- 500 Krotkov, N. A., McLinden, C. A., Li, C., Lamsal, L. N., Celarier, E. A., Marchenko, S. V., Swartz, W. H., Bucsela, E. J., Joiner, J., Duncan, B. N., Boersma, K. F., Veeckind, J. P., Levelt, P. F., Fioletov, V. E., Dickerson, R. R., He, H., Lu, Z., and Streets, D. G.: Aura OMI observations of regional SO₂ and NO₂ pollution changes from 2005 to 2015, *Atmospheric Chemistry and Physics*, 16, 4605–4629, <https://doi.org/10.5194/acp-16-4605-2016>, 2016.
- 505 Kumar, A., Pratap, V., Kumar, S., and Singh, A.: Atmospheric aerosols properties over Indo-Gangetic Plain: A trend analysis using ground – Truth AERONET data for the year 2009–2017, *Advances in Space Research*, 69, 2659–2670, <https://doi.org/10.1016/j.asr.2021.12.052>, 2022.
- Kumar, S., Singh, A., Srivastava, A. K., Sahu, S. K., Hooda, R. K., Dumka, U. C., and Pathak, V.: Long-term change in aerosol characteristics over Indo-Gangetic Basin: How significant is the impact of emerging anthropogenic activities?, *Urban Climate*, 38, 100880, <https://doi.org/10.1016/j.uclim.2021.100880>, 2021.
- 510 Kurokawa, J. and Ohara, T.: Long-term historical trends in air pollutant emissions in Asia: Regional Emission inventory in ASia (REAS) version 3, *Atmospheric Chemistry and Physics*, 20, 12 761–12 793, <https://doi.org/10.5194/acp-20-12761-2020>, 2020.
- Lee, J., Kim, J., Song, C., Kim, S., Chun, Y., Sohn, B., and Holben, B.: Characteristics of aerosol types from AERONET sunphotometer measurements, *Atmospheric Environment*, 44, 3110–3117, <https://doi.org/10.1016/j.atmosenv.2010.05.035>, 2010.
- 515 Li, J.: Pollution Trends in China from 2000 to 2017: A Multi-Sensor View from Space, *Remote Sensing*, 12, 208, <https://doi.org/10.3390/rs12020208>, 2020.
- Li, J., Carlson, B. E., Dubovik, O., and Lacis, A. A.: Recent trends in aerosol optical properties derived from AERONET measurements, *Atmospheric Chemistry and Physics*, 14, 12 271–12 289, <https://doi.org/10.5194/acp-14-12271-2014>, 2014.
- Li, J., Li, X., Carlson, B. E., Kahn, R. A., Lacis, A. A., Dubovik, O., and Nakajima, T.: Reducing multisensor satellite monthly mean aerosol optical depth uncertainty: 1. Objective assessment of current AERONET locations, *Journal of Geophysical Research: Atmospheres*, 121, <https://doi.org/10.1002/2016jd025469>, 2016.
- 520



- Li, W., Wang, Y., Yi, Z., Guo, B., Chen, W., Che, H., and Zhang, X.: Evaluation of MERRA-2 and CAMS reanalysis for black carbon aerosol in China, *Environmental Pollution*, 343, 123–182, <https://doi.org/10.1016/j.envpol.2023.123182>, 2024.
- 525 Liang, Y., Gui, K., Che, H., Li, L., Zheng, Y., Zhang, X., Zhang, X., Zhang, P., and Zhang, X.: Changes in aerosol loading before, during and after the COVID-19 pandemic outbreak in China: Effects of anthropogenic and natural aerosol, *Science of The Total Environment*, 857, 159–435, <https://doi.org/10.1016/j.scitotenv.2022.159435>, 2023.
- Mann, H. B.: Nonparametric Tests Against Trend, *Econometrica*, 13, 245, <https://doi.org/10.2307/1907187>, 1945.
- Mehta, M., Singh, R., Singh, A., Singh, N., and Anshumali: Recent global aerosol optical depth variations and trends — A comparative study using MODIS and MISR level 3 datasets, *Remote Sensing of Environment*, 181, 137–150, <https://doi.org/10.1016/j.rse.2016.04.004>, 2016.
- 530 Mishchenko, M. I., Geogdzhayev, I. V., Rossow, W. B., Cairns, B., Carlson, B. E., Laci, A. A., Liu, L., and Travis, L. D.: Long-Term Satellite Record Reveals Likely Recent Aerosol Trend, *Science*, 315, 1543–1543, <https://doi.org/10.1126/science.1136709>, 2007.
- Moorthy, K. K. and Babu, S. S.: Aerosol black carbon over Bay of Bengal observed from an island location, Port Blair: Temporal features and long-range transport, *Journal of Geophysical Research: Atmospheres*, 111, <https://doi.org/10.1029/2005jd006855>, 2006.
- Ningombam, S. S., Larson, E., Dumka, U., Estellés, V., Campanelli, M., and Steve, C.: Long-term (1995–2018) aerosol optical depth derived using ground based AERONET and SKYNET measurements from aerosol aged-background sites, *Atmospheric Pollution Research*, 10, 535 608–620, <https://doi.org/10.1016/j.apr.2018.10.008>, 2019.
- Pandey, S. K., Bakshi, H., and Vinoj, V.: Recent changes in dust and its impact on aerosol trends over the Indo-Gangetic Plain (IGP), in: *Remote Sensing of the Atmosphere, Clouds, and Precipitation VI*, edited by Im, E., Kumar, R., and Yang, S., SPIE, ISSN 0277-786X, <https://doi.org/10.1117/12.2223314>, 2016.
- 540 Pandey, S. K., Vinoj, V., Landu, K., and Babu, S. S.: Declining pre-monsoon dust loading over South Asia: Signature of a changing regional climate, *Scientific Reports*, 7, <https://doi.org/10.1038/s41598-017-16338-w>, 2017.
- Pouliot, G., van der Gon, H. A. D., Kuenen, J., Zhang, J., Moran, M. D., and Makar, P. A.: Analysis of the emission inventories and model-ready emission datasets of Europe and North America for phase 2 of the AQMEII project, *Atmospheric Environment*, 115, 345–360, <https://doi.org/10.1016/j.atmosenv.2014.10.061>, 2015.
- 545 Rafaj, P., Amann, M., Siri, J., and Wuester, H.: Changes in European greenhouse gas and air pollutant emissions 1960–2010: decomposition of determining factors, *Climatic Change*, 124, 477–504, <https://doi.org/10.1007/s10584-013-0826-0>, 2013.
- Ramachandran, S. and Rupakheti, M.: Trends in physical, optical and chemical columnar aerosol characteristics and radiative effects over South and East Asia: Satellite and ground-based observations, *Gondwana Research*, 105, 366–387, <https://doi.org/10.1016/j.gr.2021.09.016>, 2022.
- 550 Ramachandran, S., Rupakheti, M., and Lawrence, M. G.: Aerosol-induced atmospheric heating rate decreases over South and East Asia as a result of changing content and composition, *Scientific Reports*, 10, <https://doi.org/10.1038/s41598-020-76936-z>, 2020.
- Russell, P. B., Bergstrom, R. W., Shinozuka, Y., Clarke, A. D., DeCarlo, P. F., Jimenez, J. L., Livingston, J. M., Redemann, J., Dubovik, O., and Strawa, A.: Absorption Angstrom Exponent in AERONET and related data as an indicator of aerosol composition, *Atmospheric Chemistry and Physics*, 10, 1155–1169, <https://doi.org/10.5194/acp-10-1155-2010>, 2010.
- 555 Sabetghadam, S., Alizadeh, O., Khoshsima, M., and Pierleoni, A.: Aerosol properties, trends and classification of key types over the Middle East from satellite-derived atmospheric optical data, *Atmospheric Environment*, 246, 118–100, <https://doi.org/10.1016/j.atmosenv.2020.118100>, 2021.
- Sen, P. K.: Estimates of the Regression Coefficient Based on Kendall's Tau, *Journal of the American Statistical Association*, 63, 1379–1389, <https://doi.org/10.1080/01621459.1968.10480934>, 1968.



- 560 Shao, Y., Klose, M., and Wyrwoll, K.: Recent global dust trend and connections to climate forcing, *Journal of Geophysical Research: Atmospheres*, 118, <https://doi.org/10.1002/jgrd.50836>, 2013.
- Sinyuk, A., Holben, B. N., Eck, T. F., Giles, D. M., Slutsker, I., Korkin, S., Schafer, J. S., Smirnov, A., Sorokin, M., and Lyapustin, A.: The AERONET Version 3 aerosol retrieval algorithm, associated uncertainties and comparisons to Version 2, *Atmospheric Measurement Techniques*, 13, 3375–3411, <https://doi.org/10.5194/amt-13-3375-2020>, 2020.
- 565 Sokhi, R. S., Singh, V., Querol, X., Finardi, S., Targino, A. C., Andrade, M. d. F., Pavlovic, R., Garland, R. M., Massagué, J., Kong, S., Baklanov, A., Ren, L., Tarasova, O., Carmichael, G., Peuch, V.-H., Anand, V., Arbilla, G., Badali, K., Beig, G., Belalcazar, L. C., Bolignano, A., Brimblecombe, P., Camacho, P., Casallas, A., Charland, J.-P., Choi, J., Chourdakis, E., Coll, I., Collins, M., Cyrus, J., da Silva, C. M., Di Giosa, A. D., Di Leo, A., Ferro, C., Gavidia-Calderon, M., Gayen, A., Ginzburg, A., Godefroy, F., Gonzalez, Y. A., Guevara-Luna, M., Haque, S. M., Havenga, H., Herod, D., Hörrak, U., Hussein, T., Ibarra, S., Jaimes, M., Kaasik, M., Khaiwal, R., Kim, J., Kousa, A., Kukkonen, J., Kulmala, M., Kuula, J., La Violette, N., Lanzani, G., Liu, X., MacDougall, S., Manseau, P. M., Marchegiani, G., McDonald, B., Mishra, S. V., Molina, L. T., Mooibroek, D., Mor, S., Moussiopoulos, N., Murena, F., Niemi, J. V., Noe, S., Nogueira, T., Norman, M., Pérez-Camaño, J. L., Petäjä, T., Piketh, S., Rathod, A., Reid, K., Retama, A., Rivera, O., Rojas, N. Y., Rojas-Quincho, J. P., San José, R., Sánchez, O., Seguel, R. J., Sillanpää, S., Su, Y., Tapper, N., Terrazas, A., Timonen, H., Toscano, D., Tsegas, G., Velders, G. J., Vlachokostas, C., von Schneidmesser, E., VPM, R., Yadav, R., Zalakeviciute, R., and Zavala, M.: A global observational analysis to understand changes in air quality during exceptionally low anthropogenic emission conditions, *Environment International*, 157, 106 818, <https://doi.org/10.1016/j.envint.2021.106818>, 2021.
- 575 Szymankiewicz, K., Kaminski, J. W., and Struzewska, J.: Application of Satellite Observations and Air Quality Modelling to Validation of NO_x Anthropogenic EMEP Emissions Inventory over Central Europe, *Atmosphere*, 12, 1465, <https://doi.org/10.3390/atmos12111465>, 2021.
- 580 Takamura, T. and Nakajima, T.: Overview of SKYNET and its activities, *Optica pura y aplicada*, 37, 3303–3308, 2004.
- Tao, M., Wang, Z., Tao, J., Chen, L., Wang, J., Hou, C., Wang, L., Xu, X., and Zhu, H.: How Do Aerosol Properties Affect the Temporal Variation of MODIS AOD Bias in Eastern China?, *Remote Sensing*, 9, 800, <https://doi.org/10.3390/rs9080800>, 2017.
- Tong, D. Q., Lamsal, L., Pan, L., Ding, C., Kim, H., Lee, P., Chai, T., Pickering, K. E., and Stajner, I.: Long-term NO_x trends over large cities in the United States during the great recession: Comparison of satellite retrievals, ground observations, and emission inventories, *Atmospheric Environment*, 107, 70–84, <https://doi.org/10.1016/j.atmosenv.2015.01.035>, 2015.
- 585 Venkataraman, C., Brauer, M., Tibrewal, K., Sadavarte, P., Ma, Q., Cohen, A., Chaliyakunnel, S., Frostad, J., Klimont, Z., Martin, R. V., Millet, D. B., Philip, S., Walker, K., and Wang, S.: Source influence on emission pathways and ambient PM_{2.5} pollution over India (2015–2050), *Atmospheric Chemistry and Physics*, 18, 8017–8039, <https://doi.org/10.5194/acp-18-8017-2018>, 2018.
- Wang, S., Yu, Y., Zhang, X.-X., Lu, H., Zhang, X.-Y., and Xu, Z.: Weakened dust activity over China and Mongolia from 2001 to 2020 associated with climate change and land-use management, *Environmental Research Letters*, 16, 124 056, <https://doi.org/10.1088/1748-9326/ac3b79>, 2021a.
- 590 Wang, X., Cai, D., Chen, S., Lou, J., Liu, F., Jiao, L., Cheng, H., Zhang, C., Hua, T., and Che, H.: Spatio-temporal trends of dust emissions triggered by desertification in China, *CATENA*, 200, 105 160, <https://doi.org/10.1016/j.catena.2021.105160>, 2021b.
- Wei, J., Li, Z., Lyapustin, A., Sun, L., Peng, Y., Xue, W., Su, T., and Cribb, M.: Reconstructing 1-km-resolution high-quality PM_{2.5} data records from 2000 to 2018 in China: spatiotemporal variations and policy implications, *Remote Sensing of Environment*, 252, 112 136, <https://doi.org/10.1016/j.rse.2020.112136>, 2021a.



- Wei, J., Li, Z., Xue, W., Sun, L., Fan, T., Liu, L., Su, T., and Cribb, M.: The ChinaHighPM10 dataset: generation, validation, and spatiotemporal variations from 2015 to 2019 across China, *Environment International*, 146, 106 290, <https://doi.org/10.1016/j.envint.2020.106290>, 2021b.
- 600 Wu, C., Lin, Z., Shao, Y., Liu, X., and Li, Y.: Drivers of recent decline in dust activity over East Asia, *Nature Communications*, 13, <https://doi.org/10.1038/s41467-022-34823-3>, 2022.
- Xia, X.: Variability of aerosol optical depth and Angstrom wavelength exponent derived from AERONET observations in recent decades, *Environmental Research Letters*, 6, 044 011, <https://doi.org/10.1088/1748-9326/6/4/044011>, 2011.
- Yang, X., Zhao, C., Yang, Y., and Fan, H.: Long-term multi-source data analysis about the characteristics of aerosol optical properties and types over Australia, *Atmospheric Chemistry and Physics*, 21, 3803–3825, <https://doi.org/10.5194/acp-21-3803-2021>, 2021.
- 605 Yin, S.: Biomass burning spatiotemporal variations over South and Southeast Asia, *Environment International*, 145, 106 153, <https://doi.org/10.1016/j.envint.2020.106153>, 2020.
- Ying, T., Li, J., Jiang, Z., Liu, G., Zhang, Z., Zhang, L., Dong, Y., and Zhao, C.: Increased aerosol scattering contributes to the recent monsoon rainfall decrease over the Gangetic Plain, *Science Bulletin*, 68, 2629–2638, <https://doi.org/10.1016/j.scib.2023.08.052>, 2023.
- 610 Yoon, J., von Hoyningen-Huene, W., Kokhanovsky, A. A., Vountas, M., and Burrows, J. P.: Trend analysis of aerosol optical thickness and Ångström exponent derived from the global AERONET spectral observations, *Atmospheric Measurement Techniques*, 5, 1271–1299, <https://doi.org/10.5194/amt-5-1271-2012>, 2012.
- Yoon, J., Pozzer, A., Chang, D., Lelieveld, J., Kim, J., Kim, M., Lee, Y., Koo, J.-H., Lee, J., and Moon, K.: Trend estimates of AERONET-observed and model-simulated AOTs between 1993 and 2013, *Atmospheric Environment*, 125, 33–47, <https://doi.org/10.1016/j.atmosenv.2015.10.058>, 2016.
- 615 Yu, X., Nichol, J., Lee, K. H., Li, J., and Wong, M. S.: Analysis of Long-Term Aerosol Optical Properties Combining AERONET Sunphotometer and Satellite-Based Observations in Hong Kong, *Remote Sensing*, 14, 5220, <https://doi.org/10.3390/rs14205220>, 2022.
- Zhang, L. and Li, J.: Variability of Major Aerosol Types in China Classified Using AERONET Measurements, *Remote Sensing*, 11, 2334, <https://doi.org/10.3390/rs11202334>, 2019.
- 620 Zhang, Y., Luo, G., and Yu, F.: Seasonal Variations and Long-Term Trend of Dust Particle Number Concentration Over the Northeastern United States, *Journal of Geophysical Research: Atmospheres*, 124, 13 140–13 155, <https://doi.org/10.1029/2019jd031388>, 2019.
- Zhang, Y., Cai, Y.-J., Yu, F., Luo, G., and Chou, C. C.: Seasonal Variations and Long-term Trend of Mineral Dust Aerosols over the Taiwan Region, *Aerosol and Air Quality Research*, 21, 200 433, <https://doi.org/10.4209/aaqr.2020.07.0433>, 2021.
- Zhang, Z., Li, J., Dong, Y., Zhang, C., Ying, T., and Li, Q.: Long-term trends in aerosol single scattering albedo cause bias in MODIS aerosol optical depth trends, *IEEE Transactions on Geoscience and Remote Sensing*, pp. 1–1, <https://doi.org/10.1109/tgrs.2024.3424981>, 2024.
- 625 Zhao, B., Jiang, J. H., Gu, Y., Diner, D., Worden, J., Liou, K.-N., Su, H., Xing, J., Garay, M., and Huang, L.: Decadal-scale trends in regional aerosol particle properties and their linkage to emission changes, *Environmental Research Letters*, 12, 054 021, <https://doi.org/10.1088/1748-9326/aa6cb2>, 2017.
- Zhao, Y., Xin, Z., and Ding, G.: Spatiotemporal variation in the occurrence of sand-dust events and its influencing factors in the Beijing-Tianjin Sand Source Region, China, 1982–2013, *Regional Environmental Change*, 18, 2433–2444, <https://doi.org/10.1007/s10113-018-1365-z>, 2018.
- 630